CERN-PH-TH/2005-078
hep-ph/0505018

New Physics in B and K Decays

Robert Fleischer
CERN, Department of Physics, Theory Unit
CH-1211 Geneva 23, Switzerland

Abstract

Flavour physics offers interesting probes for the exploration of the Standard Model and the search for new physics. In these lectures, we focus on B- and K-meson decays, introduce the concept of low-energy effective Hamiltonians to describe them theoretically, and discuss how physics beyond the Standard Model may generically affect the roadmap of quark-flavour physics. We address then both the implications of the B-factory data for the $B_d \to J/\psi K_{\rm S}$ channel and the prospects of $B_s \to J/\psi\phi$ modes for hadron colliders, and discuss how the Standard Model may be challenged through $B_d \to \phi K_{\rm S}$. Finally, as an example of a systematic flavour strategy to search for new physics, we analyze puzzling patterns in the $B \to \pi\pi, \pi K$ data and study their interplay with rare K and B decays.

Invited lectures given at the Lake Louise Winter Institute:
"Fundamental Interactions"
Chateau Lake Louise, Alberta, Canada, 20–26 February 2005
To appear in the Proceedings (World Scientific)

CERN-PH-TH/2005-078
May 2005

NEW PHYSICS IN B AND K DECAYS

R. FLEISCHER
CERN, Department of Physics, Theory Unit,
CH-1211 Geneva 23, Switzerland
E-mail: Robert.Fleischer@cern.ch

Flavour physics offers interesting probes for the exploration of the Standard Model and the search for new physics. In these lectures, we focus on B- and K-meson decays, introduce the concept of low-energy effective Hamiltonians to describe them theoretically, and discuss how physics beyond the Standard Model may generically affect the roadmap of quark-flavour physics. We address then both the implications of the B-factory data for the $B_d \to J/\psi K_{\rm S}$ channel and the prospects of $B_s \to J/\psi\phi$ modes for hadron colliders, and discuss how the Standard Model may be challenged through $B_d \to \phi K_{\rm S}$. Finally, as an example of a systematic flavour strategy to search for new physics, we analyze puzzling patterns in the $B \to \pi\pi, \pi K$ data and study their interplay with rare K and B decays.

1. Introduction

In flavour physics, the parity and charge-conjugation operators $\hat{P}$ and $\hat{C}$, which describe the space-inversion operation and the replacement of all particles by their antiparticles, respectively, play a key rôle. After the discovery that weak interactions are not invariant under parity and charge-conjugation transformations in 1957, it was believed that the product of $\hat{C}$ and $\hat{P}$ was actually preserved. It came then as a big surprise in 1964,[1] when it was observed through the detection of $K_{\rm L} \to \pi^+\pi^-$ decays that this is actually *not* the case! The corresponding phenomenon is referred to as *CP violation*, and is a central aspect of flavour physics. The manifestation of CP violation discovered in 1964 is "indirect" CP violation, which is described by a complex quantitiy ε_K and originates from the fact that the mass eigenstates of the neutral kaons are not eigenstates of the CP operator. After tremendous experimental efforts, also "direct" CP violation, which is caused *directly* at the amplitude level through the interference between different weak amplitudes, could be established in the neutral kaon system in 1999 by the NA48 (CERN) and KTeV (FNAL) collaborations,[2] thereby ruling out superweak scenarios of CP violation.[3] The world average taking

also the final NA48 and KTeV results[4] into account is given as follows:

$$\mathrm{Re}(\varepsilon'/\varepsilon) = (16.6 \pm 1.6) \times 10^{-4}. \tag{1}$$

As far as the theoretical status of this observable is concerned, the short-distance contributions are under full control. On the other hand, the long-distance part, which is described by hadronic matrix elements of certain four-quark operators, suffers from large uncertainties. Although theoretical analyses performed within the Standard Model give results in the ball park of (1), stringent tests cannot be performed unless progress on the long-distance contributions can be made.[5]

In 2001, CP-violating effects were also discovered in the B-meson system by the BaBar (SLAC) and Belle (KEK) collaborations,[6] representing the first observation of this phenomenon *outside* the K-meson system. The corresponding CP asymmetry arises in the "golden" decay $B_d \to J/\psi K_S$,[7] and is induced through the interference between the $B_d^0 \to J/\psi K_S$ and $\bar{B}_d^0 \to J/\psi K_S$ decay processes that is caused by B_d^0–$\bar{B}_d^0$ mixing. In the summer of 2004, also direct CP violation could be detected by the BaBar and Belle collaborations in $B_d \to \pi^\mp K^\pm$ decays,[8] thereby complementing the observation of this phenomenon in the neutral kaon system.

Despite tremendous progress over the last years, we have still an incomplete picture of CP violation and flavour physics. The exploration of these topics is very exciting, as it may open a window to the physics lying beyond the Standard Model (SM), where quark-flavour physics is governed by the Cabibbo–Kobayashi–Maskawa (CKM) matrix.[9,10] Indeed, in scenarios for new physics (NP), we typically encounter also new sources for flavour-changing processes and CP violation. Important examples are models with extended Higgs sectors, supersymmetric (SUSY) or left–right-symmetric scenarios for NP. In this context, it is also important to note that the experimental evidence for non-vanishing neutrino masses points to an origin beyond the SM, raising many interesting questions, which include also the possibility of CP violation in the neutrino sector.[11]

Interestingly, CP violation plays also an outstanding rôle in cosmology, where this phenomenon is one of the necessary ingredients for the generation of the matter–antimatter asymmetry of the Universe,[12] as was pointed out by Sakharov in 1967.[13] However, model calculations show that the CP violation present in the SM is too small to explain this asymmetry. The required additional sources of CP violation may be associated with very high energy scales, as in the scenario of "leptogenesis", involving CP-violating decays of very heavy Majorana neutrinos.[14] On the other hand, there are

also several extensions of the SM with new sources of CP violation that could actually be accessible in the laboratory, as we have noted above.

Before searching for NP, we have first to understand the picture of flavour physics emerging within the SM. Here the usual key problem for the theoretical interpretation is related to hadronic uncertainties, where ε'/ε is a famous example. In the B-meson system, the situation is much more promising: it offers various strategies to explore CP violation and flavour physics – simply speaking, there are *many* B decays – and we may search for SM relations, which are on solid theoretical ground and may well be affected by NP. Concerning the kaon system, the future lies on "rare" decays, which are absent at the tree level of the SM, i.e. originate from loop processes, and are theoretically very clean. A particularly important rôle is played by $K^+ \to \pi^+\nu\bar{\nu}$ and $K_{\rm L} \to \pi^0\nu\bar{\nu}$, which offer poweful tests of the flavour sector of the SM.

These aspects are the focus of these lectures. The outline is as follows: in Section 2, we discuss the description of CP violation in the SM and introduce the unitarity triangle(s). We then move on to the system of the B mesons in Section 3, where we classify non-leptonic B decays, introduce the concept of low-energy effective Hamiltonians, and have a closer look at the CP-violating asymmetries arising in neutral B decays. In Section 4, we turn to rare decays, and discuss $B_{s,d} \to \mu^+\mu^-$ modes as a more detailed example. After addressing the question of how NP may generically enter CP-violating phenomena and rare decays in Section 5, we are well prepared to discuss the "golden" decays $B_d \to J/\psi K_{\rm S}$ and $B_s \to J/\psi\phi$ in Section 6, and how we may challenge the SM through $B_d \to \phi K_{\rm S}$ modes in Section 7. In Section 8, we consider an example of a systematic strategy to search for NP, which is an an analysis of puzzling patterns in the $B \to \pi\pi, \pi K$ data and their interplay with rare K and B decays. Finally, we conclude and give a brief outlook in Section 9.

In order to complement the discussion given here, I refer the reader to the reviews, lecture notes and textbooks collected in Refs. 15–21, where many more details and different perspectives of the field can be found. There are also other fascinating aspects of flavour physics and CP violation, which are, however, beyond the scope of these lectures. Important examples are the D-meson system,[22] electric dipole moments,[23] or the search for flavour-violating charged lepton decays.[24] In order to get an overview of these topics, the reader should consult the corresponding references.

2. CP Violation in the Standard Model

2.1. *Weak Interactions of Quarks*

In the SM of electroweak interactions, CP-violating effects are associated with the charged-current interactions of the quarks:

$$D \to U W^- . \tag{2}$$

Here $D \in \{d, s, b\}$ and $U \in \{u, c, t\}$ denote down- and up-type quark flavours, respectively, whereas the W^- is the usual $SU(2)_{\rm L}$ gauge boson. From a phenomenological point of view, it is convenient to collect the generic "coupling strengths" V_{UD} of the charged-current processes in (2) in the form of a 3×3 matrix. From a theoretical point of view, this "quark-mixing" matrix – the CKM matrix – connects the electroweak states (d', s', b') of the down, strange and bottom quarks with their mass eigenstates (d, s, b) through the following unitary transformation :

$$\begin{pmatrix} d' \\ s' \\ b' \end{pmatrix} = \begin{pmatrix} V_{ud} & V_{us} & V_{ub} \\ V_{cd} & V_{cs} & V_{cb} \\ V_{td} & V_{ts} & V_{tb} \end{pmatrix} \cdot \begin{pmatrix} d \\ s \\ b \end{pmatrix} \equiv \hat{V}_{\rm CKM} \cdot \begin{pmatrix} d \\ s \\ b \end{pmatrix} . \tag{3}$$

Consequently, $\hat{V}_{\rm CKM}$ is actually a *unitary* matrix. This feature ensures the absence of flavour-changing neutral-current (FCNC) processes at the tree level in the SM, and is hence at the basis of the Glashow–Iliopoulos–Maiani (GIM) mechanism.[25] If we express the non-leptonic charged-current interaction Lagrangian in terms of the mass eigenstates in (3), we arrive at

$$L_{\rm int}^{\rm CC} = -\frac{g_2}{\sqrt{2}} \left(\bar{u}_{\rm L}, \bar{c}_{\rm L}, \bar{t}_{\rm L} \right) \gamma^\mu \, \hat{V}_{\rm CKM} \begin{pmatrix} d_{\rm L} \\ s_{\rm L} \\ b_{\rm L} \end{pmatrix} W_\mu^\dagger \; + \; \text{h.c.}, \tag{4}$$

where g_2 is the $SU(2)_{\rm L}$ gauge coupling, and the $W_\mu^{(\dagger)}$ field corresponds to the charged W bosons. Looking at the interaction vertices following from (4), we observe that the elements of the CKM matrix describe in fact the generic strengths of the associated charged-current processes, as we have noted above.

Since the CKM matrix elements governing a $D \to U W^-$ transition and its CP conjugate $\bar{D} \to \bar{U} W^+$ are related to each other through

$$V_{UD} \xrightarrow{CP} V_{UD}^* , \tag{5}$$

we observe that CP violation is associated with complex phases of the CKM matrix. Consequently, the question of whether we may actually have *physical* complex phases in this matrix arises.

2.2. *Phase Structure of the CKM Matrix*

We may redefine the up- and down-type quark fields as follows:

$$U \to \exp(i\xi_U)U, \quad D \to \exp(i\xi_D)D. \tag{6}$$

If we perform such transformations in (4), the invariance of the charged-current interaction Lagrangian implies

$$V_{UD} \to \exp(i\xi_U)V_{UD}\exp(-i\xi_D). \tag{7}$$

Eliminating unphysical phases through these transformations, we are left with the following parameters in the case of a general $N \times N$ quark-mixing matrix, where N denotes the number of fermion generations:

$$\underbrace{\frac{1}{2}N(N-1)}_{\text{Euler angles}} + \underbrace{\frac{1}{2}(N-1)(N-2)}_{\text{complex phases}} = (N-1)^2. \tag{8}$$

If we apply this expression to $N = 2$ generations, we observe that only one rotation angle – the Cabibbo angle $\theta_{\rm C}$[9] – is required for the parametrization of the 2×2 quark-mixing matrix, which can be written as

$$\hat{V}_{\rm C} = \begin{pmatrix} \cos\theta_{\rm C} & \sin\theta_{\rm C} \\ -\sin\theta_{\rm C} & \cos\theta_{\rm C} \end{pmatrix}, \tag{9}$$

where $\sin\theta_{\rm C} = 0.22$ follows from $K \to \pi\ell\bar{\nu}_\ell$ decays. On the other hand, in the case of $N = 3$ generations, the parametrization of the corresponding 3×3 quark-mixing matrix involves three Euler-type angles and a single *complex* phase. This complex phase allows us to accommodate CP violation in the SM, as was pointed out by Kobayashi and Maskawa in 1973.[10] The corresponding picture is referred to as the Kobayashi–Maskawa (KM) mechanism of CP violation.

In the "standard parametrization" advocated by the Particle Data Group,[26] the three-generation CKM matrix takes the following form:

$$\hat{V}_{\rm CKM} = \begin{pmatrix} c_{12}c_{13} & s_{12}c_{13} & s_{13}e^{-i\delta_{13}} \\ -s_{12}c_{23} - c_{12}s_{23}s_{13}e^{i\delta_{13}} & c_{12}c_{23} - s_{12}s_{23}s_{13}e^{i\delta_{13}} & s_{23}c_{13} \\ s_{12}s_{23} - c_{12}c_{23}s_{13}e^{i\delta_{13}} & -c_{12}s_{23} - s_{12}c_{23}s_{13}e^{i\delta_{13}} & c_{23}c_{13} \end{pmatrix}, \tag{10}$$

where $c_{ij} \equiv \cos\theta_{ij}$ and $s_{ij} \equiv \sin\theta_{ij}$. If we redefine the quark-field phases appropriately, θ_{12}, θ_{23} and θ_{13} can all be made to lie in the first quadrant. The advantage of this parametrization is that the mixing between two generations i and j vanishes if θ_{ij} is set to zero. In particular, for $\theta_{23} = \theta_{13} = 0$, the third generation decouples, and the submatrix describing the mixing between the first and second generations takes the same form as (9).

2.3. *Wolfenstein Parametrization*

The charged-current interactions of the quarks exhibit an interesting hierarchy, which follows from experimental data:[26] transitions within the same generation involve CKM matrix elements of $O(1)$, those between the first and the second generation are associated with CKM elements of $O(10^{-1})$, those between the second and the third generation are related to CKM elements of $O(10^{-2})$, and those between the first and third generation are described by CKM matrix elements of $O(10^{-3})$. For phenomenological applications, it would be useful to have a parametrization of the CKM matrix available that makes this pattern explicit.[27] To this end, we introduce a set of new parameters, λ, A, ρ and η, by imposing the following relations:[28]

$$s_{12} \equiv \lambda = 0.22, \quad s_{23} \equiv A\lambda^2, \quad s_{13}e^{-i\delta_{13}} \equiv A\lambda^3(\rho - i\eta). \tag{11}$$

Going back to the standard parametrization (10), we obtain an *exact* parametrization of the CKM matrix as a function of λ (and A, ρ, η), which allows us to expand each CKM element in powers of the small parameter λ. Neglecting terms of $O(\lambda^4)$ yields the "Wolfenstein parametrization":[27]

$$\hat{V}_{\rm CKM} = \begin{pmatrix} 1 - \frac{1}{2}\lambda^2 & \lambda & A\lambda^3(\rho - i\eta) \\ -\lambda & 1 - \frac{1}{2}\lambda^2 & A\lambda^2 \\ A\lambda^3(1 - \rho - i\eta) & -A\lambda^2 & 1 \end{pmatrix} + O(\lambda^4). \tag{12}$$

2.4. *Unitarity Triangle(s)*

The unitarity of the CKM matrix, which is described by

$$\hat{V}_{\rm CKM}^{\dagger} \cdot \hat{V}_{\rm CKM} = \hat{1} = \hat{V}_{\rm CKM} \cdot \hat{V}_{\rm CKM}^{\dagger}, \tag{13}$$

leads to a set of 12 equations, consisting of 6 normalization and 6 orthogonality relations. The latter can be represented as 6 triangles in the complex plane, all having the same area, which represents a measure of the "strenghth" of CP violation in the SM.

Using the Wolfenstein parametrization of the CKM matrix, the generic shape of these triangles can be explored. Interestingly, only the following two orthogonality relations correspond to the case of triangles, where all three sides are of the same order of magnitude:

$$V_{ud}V_{ub}^* + V_{cd}V_{cb}^* + V_{td}V_{tb}^* = 0 \tag{14}$$

$$V_{ud}^*V_{td} + V_{us}^*V_{ts} + V_{ub}^*V_{tb} = 0; \tag{15}$$

in the other triangles, one side is suppressed with respect to the others by factors of $O(\lambda^2)$ or $O(\lambda^4)$. If we apply the Wolfenstein parametrization by

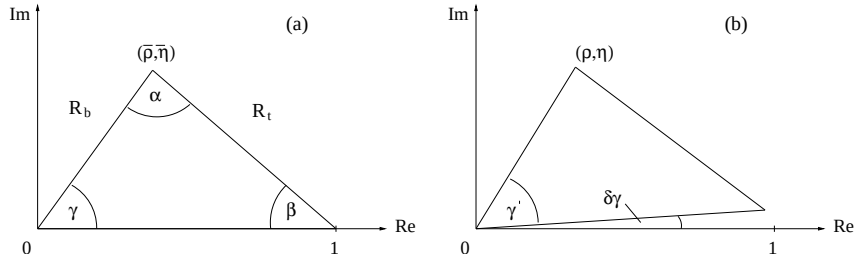

Figure 1. The two non-squashed unitarity triangles of the CKM matrix, as explained in the text: (a) and (b) correspond to the orthogonality relations (14) and (15), respectively.

keeping just the leading, non-vanishing terms of the expansion in λ, (14) and (15) give the same result, which is given by

$$[(\rho + i\eta) + (1 - \rho - i\eta) + (-1)]\, A\lambda^3 = 0, \tag{16}$$

and describes *the* unitarity triangle of the CKM matrix. Taking also the next-to-leading order corrections in λ into account,[28] as described in Subsection 2.3, we arrive at the triangles illustrated in Fig. 1. The apex of the triangle in Fig. 1 (a) is simply given by

$$\bar{\rho} \equiv \rho \left[1 - \frac{1}{2}\lambda^2\right], \quad \bar{\eta} \equiv \eta \left[1 - \frac{1}{2}\lambda^2\right], \tag{17}$$

corresponding to the triangle sides

$$R_b \equiv \left[1 - \frac{\lambda^2}{2}\right] \frac{1}{\lambda} \left|\frac{V_{ub}}{V_{cb}}\right|, \quad R_t \equiv \frac{1}{\lambda} \left|\frac{V_{td}}{V_{cb}}\right|. \tag{18}$$

Obviously, this triangle is the straightforward generalization of the leading-order case, and is usually considered in the literature. Whenever referring to *a* unitarity triangle (UT) in the following discussion, we shall always mean this triangle. On the other hand, the characteristic feature of the triangle in Fig. 1 (b) is that $\gamma = \gamma' + \delta\gamma$, with

$$\delta\gamma = \lambda^2\eta = O(1^\circ). \tag{19}$$

2.5. *Determination of the Unitarity Triangle*

There are two conceptually different avenues to determine the UT:

(i) In the "CKM fits", theory is used to convert experimental data into contours in the $\bar{\rho}$–$\bar{\eta}$ plane, where semileptonic $b \to u\ell\bar{\nu}_\ell$, $c\ell\bar{\nu}_\ell$ decays and $B^0_{d,s}$–$\bar{B}^0_{d,s}$ mixing (see 3.1) allow us to determine the

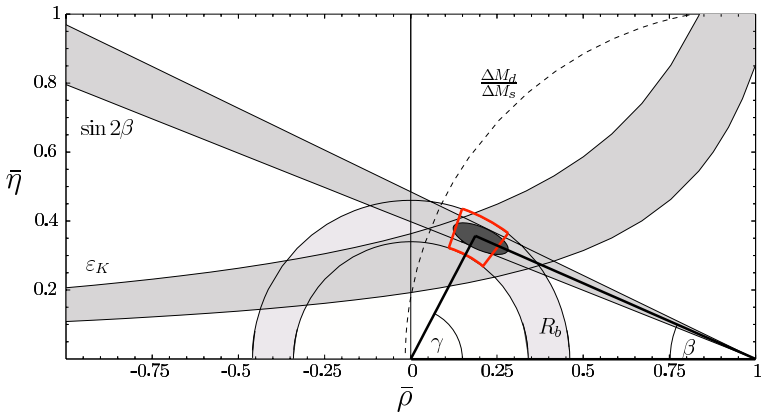

Figure 2. The current situation in the $\bar{\rho}$–$\bar{\eta}$ plane, as discussed in the text.

UT sides R_b and R_t, respectively, i.e. to fix two circles in the $\bar{\rho}$–$\bar{\eta}$ plane. On the other hand, the indirect CP violation in the neutral kaon system described by ε_K can be transformed into a hyperbola.

(ii) Theory allows us to convert measurements of CP-violating effects in B-meson decays into direct information on the UT angles. The most prominent example is the determination of $\sin 2\beta$ through $B_d \to J/\psi K_S$, but several other strategies were proposed.

The goal is to "overconstrain" the UT as much as possible. In the future, additional contours can be fixed in the $\bar{\rho}$–$\bar{\eta}$ plane through the measurement of rare decays. For example, $\mathrm{BR}(K^+ \to \pi^+ \nu\bar{\nu})$ can be converted into an ellipse, and $\mathrm{BR}(K_L \to \pi^0 \nu\bar{\nu})$ allows the determination of $|\bar{\eta}|$.

In Fig. 2, we show the current situation: the shaded dark ellipse is the result of a CKM fit,[29] the straight lines represent the measurement of $\sin 2\beta$ (see Subsection 6.1), and the quadrangle corresponds to a determination of γ from $B_d \to \pi^+\pi^-$, $B_d \to \pi^\mp K^\pm$ decays,[30] which will be discussed in Section 8. For very comprehensive analyses of the UT, we refer the reader to the web sites of the "CKM Fitter Group" and the "UTfit collaboration".[31]

The overall consistency with the SM is very impressive. Furthermore, also the recent data for $B \to \pi\rho, \rho\rho$ as well as $B_d \to D^{(*)\pm}\pi^\mp$ and $B \to DK$ decays give constraints for the UT that are in accordance with the KM mechanism, although the errors are still pretty large in several of these cases. Despite this remarkably consistent picture, there is still hope to encounter deviations from the SM. Since B mesons play a key rôle in this adventure, let us next have a closer look at them.

3. System of the B Mesons

3.1. *Basic Features*

In this decade, there are promising perspectives for the exploration of B-meson decays: the asymmetric e^+–e^- B factories at SLAC and KEK, with their detectors BaBar and Belle, respectively, are taking data since several years and could already produce $O(10^8)$ $B\bar{B}$ pairs. Moreover, the CDF and D0 collaborations have recently reported the first results from run II of Fermilab's Tevatron. Starting in 2007, the LHC[32] at CERN will allow "second-generation" B-decay studies through the dedicated LHCb experiment, and also ATLAS and CMS can address certain interesting aspects of B physics. For the more distant future, an e^+–e^- "super-B factory" is under consideration, with an increase of luminosity by two orders of magnitude with respect to the currently operating machines.[33]

The B-meson system offers also a very interesting playground for theorists, involving exciting aspects of strong and weak interactions, as well as the possible impact of physics beyond the SM. Moreover, there is an extremely fruitful interplay between theory and experiment in this field, and despite impressive progress, there are still aspects left that could not yet be accessed experimentally and are essentially unexplored.

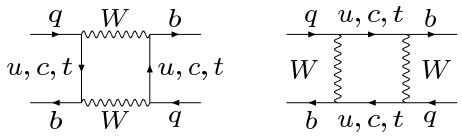

Figure 3. Box diagrams contributing to B^0_q–$\bar{B}^0_q$ mixing in the SM ($q \in \{d, s\}$).

The B-meson system consists of charged and neutral mesons, which are characterized by the following valence-quark contents:

$$\text{charged: } \begin{bmatrix} B^+ \sim u\,\bar{b}, & B^- \sim \bar{u}\,b \\ B_c^+ \sim c\,\bar{b}, & B_c^+ \sim \bar{c}\,b \end{bmatrix}, \quad \text{neutral: } \begin{bmatrix} B_d^0 \sim d\,\bar{b}, & \bar{B}_d^0 \sim \bar{d}\,b \\ B_s^0 \sim s\,\bar{b}, & \bar{B}_s^0 \sim \bar{s}\,b \end{bmatrix}.$$

The characteristic feature of the neutral B_q ($q \in \{d, s\}$) mesons is B^0_q–$\bar{B}^0_q$ mixing, which we encountered already in the determination of the UT discussed in Subsection 2.5. In the SM, this phenomenon, which is the counterpart of K^0–$\bar{K}^0$ mixing, originates from box diagrams, as illustrated in Fig. 3. Due to B^0_q–$\bar{B}^0_q$ mixing, an initially, i.e. at time $t = 0$, present B^0_q-meson state evolves into the following time-dependent linear combination:

$$|B_q(t)\rangle = a(t)|B^0_q\rangle + b(t)|\bar{B}^0_q\rangle. \tag{20}$$

The coefficients $a(t)$ and $b(t)$ are governed by an appropriate Schrödinger equation, with mass eigenstates that are characterized by mass and decay width differences ΔM_q and $\Delta\Gamma_q$, respectively. The time-dependent transition rates for decays of initially present B_q^0 or $\bar{B}_q^0$ mesons into a final state f involve $\cos(\Delta M_q t)$ and $\sin(\Delta M_q t)$ terms, describing the B_q^0–$\bar{B}_q^0$ oscillations.

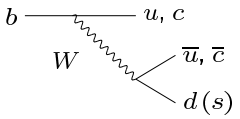

Figure 4. Tree diagrams ($q_1, q_2 \in \{u, c\}$).

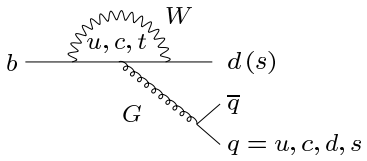

Figure 5. QCD penguin diagrams ($q_1 = q_2 \in \{u, d, c, s\}$).

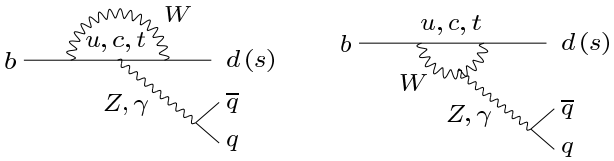

Figure 6. Electroweak penguin diagrams ($q_1 = q_2 \in \{u, d, c, s\}$).

3.2. *Classification of Non-Leptonic B Decays*

For the exploration of CP violation, non-leptonic B decays play the key rôle. The final states of such transitions consist only of quarks, and they are mediated by $b \to q_1\,\bar{q}_2\,d\,(s)$ quark-level processes, with $q_1, q_2 \in \{u, d, c, s\}$. There are two kinds of topologies contributing to such decays: "tree" and "penguin" topologies. The latter consist of gluonic (QCD) and electroweak (EW) penguins. In Figs. 4–6, the corresponding leading-order Feynman diagrams are shown. Depending on the flavour content of their final states, we may classify the non-leptonic $b \to q_1\,\bar{q}_2\,d\,(s)$ decays as follows:

- $q_1 \neq q_2 \in \{u, c\}$: *only* tree diagrams contribute.
- $q_1 = q_2 \in \{u, c\}$: tree *and* penguin diagrams contribute.
- $q_1 = q_2 \in \{d, s\}$: *only* penguin diagrams contribute.

3.3. *Low-Energy Effective Hamiltonians*

3.3.1. *General Structure*

For the analysis of non-leptonic B decays, we use low-energy effective Hamiltonians, which are calculated by making use of the "operator product expansion", yielding transition amplitudes of the following structure:

$$\langle f|H_{\rm eff}|i\rangle = \frac{G_{\rm F}}{\sqrt{2}}\lambda_{\rm CKM}\sum_k C_k(\mu)\langle f|Q_k(\mu)|i\rangle. \tag{21}$$

Here $G_{\rm F}$ denotes Fermi's constant, $\lambda_{\rm CKM}$ is a CKM factor, and μ denotes a renormalization scale. The technique of the operator product expansion allows us to separate the short-distance contributions to this transition amplitude from the long-distance ones, which are described by perturbative quantities $C_k(\mu)$ ("Wilson coefficient functions") and non-perturbative quantities $\langle f|Q_k(\mu)|i\rangle$ ("hadronic matrix elements"), respectively. The Q_k are local operators, which are generated through the electroweak interactions and the interplay with QCD, and govern "effectively" the decay in question. The Wilson coefficients are – simply speaking – the scale-dependent couplings of the vertices described by the Q_k.

3.3.2. *Illustration through an Example*

Let us consider the quark-level process $b \to c\bar{u}s$, which originates from a tree diagram of the kind shown in Fig. 4, as a simple illustration. If we "integrate out" the W boson having four-momentum k, i.e. use the relation

$$\frac{g_{\nu\mu}}{k^2 - M_W^2} \quad \stackrel{k^2 \ll M_W^2}{\longrightarrow} \quad -\frac{g_{\nu\mu}}{M_W^2} \equiv -\left(\frac{8G_{\rm F}}{\sqrt{2}g_2^2}\right) g_{\nu\mu}, \tag{22}$$

we arrive at the following low-energy effective Hamiltonian:

$$H_{\rm eff} = \frac{G_{\rm F}}{\sqrt{2}} V_{us}^* V_{cb} O_2, \tag{23}$$

with the "current–current" operator

$$O_2 \equiv [\bar{s}_\alpha \gamma_\mu (1-\gamma_5) u_\alpha]\,[\bar{c}_\beta \gamma^\mu (1-\gamma_5) b_\beta] \tag{24}$$

and the Wilson coefficient $C_2 = 1$; α and β are the $SU(3)_{\rm C}$ indices of QCD. Taking now QCD effects, i.e. the exchange of gluons, into account and performing a proper "matching" between the full and the effective theories, a second current–current operator,

$$O_1 \equiv [\bar{s}_\alpha \gamma_\mu (1-\gamma_5) u_\beta]\,[\bar{c}_\beta \gamma^\mu (1-\gamma_5) b_\alpha]\,, \tag{25}$$

is generated, involving a Wilson coefficient $C_1(\mu)$. Due to the impact of QCD, also the Wilson coefficient of O_2 acquires now a renormalization-scale dependence and deviates from one. The results for the $C_k(\mu)$ contain terms of $\log(\mu/M_W)$, which become large for $\mu = O(m_b)$, the typical scale governing the hadronic matrix elements of the four-quark operators O_k. In order to deal with these large logarithms, "renormalization-group-improved" perturbation theory offers the appropriate tool. The fact that $\langle f|H_{\rm eff}|i\rangle$ in (21) *cannot* depend on the renormalization scale μ implies a renormalization group equation, which has a solution of the following form:

$$\vec{C}(\mu) = \hat{U}(\mu, M_W) \cdot \vec{C}(M_W). \tag{26}$$

Here the "evolution matrix" $\hat{U}(\mu, M_W)$ connects the initial values $\vec{C}(M_W)$ encoding the whole *short-distance* physics at high-energy scales with the coefficients at scales at the level of a few GeV. Following these lines,

$$\alpha_s^n \left[\log\left(\frac{\mu}{M_W}\right)\right]^n \text{(LO)}, \quad \alpha_s^n \left[\log\left(\frac{\mu}{M_W}\right)\right]^{n-1} \text{(NLO)}, \quad ... \tag{27}$$

can be systematically summed up, where "LO" and "NLO" stand for the leading and next-to-leading order approximations, respectively. For more detailed discussions, we refer the reader to Refs. 17, 34.

3.3.3. *A Closer Look at Non-Leptonic Decays*

Low-energy effective Hamiltonians provide a general tool for the theoretical description of weak B- and K-meson decays, as well as B_q^0–$\bar{B}_q^0$ and K^0–$\bar{K}^0$ mixing. Let us discuss the application to non-leptonic B decays in more detail. For the exploration of CP violation, transitions with $\Delta C = \Delta U = 0$ are particularly interesting. As can be seen from Figs. 4–6, these decays receive contributions both from tree and from penguin topologies. If we apply the unitarity of the CKM matrix, we find that the corresponding CKM factors are related through

$$V_{ur}^* V_{ub} + V_{cr}^* V_{cb} + V_{tr}^* V_{tb} = 0, \tag{28}$$

where $r \in \{d, s\}$. Consequently, only *two* independent weak amplitudes contribute to any given decay of this kind. In comparison with our previous example, which was a pure tree decay, we have now also to deal with penguin topologies, involving – in addition to the W boson – the top quark as a second "heavy" particle. Once these degrees of freedom are "integrated out", their influence is only felt through the initial conditions of the renormalization group evolution (26). Mathematically, the penguin topologies

in Figs. 5 and 6 with internal top-quark exchanges (as well as the corresponding box diagrams in Fig. 3) that enter these coefficients are described by certain "Inami–Lim functions".[35] Finally, using (28) to eliminate $V_{tr}^* V_{tb}$, we obtain an effective Hamiltonian of the following structure:

$$H_{\text{eff}} = \frac{G_{\text{F}}}{\sqrt{2}} \left[\sum_{j=u,c} V_{jr}^* V_{jb} \left\{ \sum_{k=1}^{2} C_k(\mu)\, Q_k^{jr} + \sum_{k=3}^{10} C_k(\mu)\, Q_k^r \right\} \right]. \tag{29}$$

Here we have introduced another quark-flavour label $j \in \{u, c\}$, and the four-quark operators Q_k^{jr} can be divided as follows:

- Current–current operators:

$$\begin{array}{l} Q_1^{jr} = (\bar{r}_\alpha j_\beta)_{\text{V–A}} (\bar{j}_\beta b_\alpha)_{\text{V–A}} \\ Q_2^{jr} = (\bar{r}_\alpha j_\alpha)_{\text{V–A}} (\bar{j}_\beta b_\beta)_{\text{V–A}}. \end{array} \tag{30}$$

- QCD penguin operators:

$$\begin{array}{l} Q_3^r = (\bar{r}_\alpha b_\alpha)_{\text{V–A}} \sum_{q'} (\bar{q}'_\beta q'_\beta)_{\text{V–A}} \\ Q_4^r = (\bar{r}_\alpha b_\beta)_{\text{V–A}} \sum_{q'} (\bar{q}'_\beta q'_\alpha)_{\text{V–A}} \\ Q_5^r = (\bar{r}_\alpha b_\alpha)_{\text{V–A}} \sum_{q'} (\bar{q}'_\beta q'_\beta)_{\text{V+A}} \\ Q_6^r = (\bar{r}_\alpha b_\beta)_{\text{V–A}} \sum_{q'} (\bar{q}'_\beta q'_\alpha)_{\text{V+A}}. \end{array} \tag{31}$$

- EW penguin operators (the $e_{q'}$ denote the electrical quark charges):

$$\begin{array}{l} Q_7^r = \frac{3}{2} (\bar{r}_\alpha b_\alpha)_{\text{V–A}} \sum_{q'} e_{q'} (\bar{q}'_\beta q'_\beta)_{\text{V+A}} \\ Q_8^r = \frac{3}{2} (\bar{r}_\alpha b_\beta)_{\text{V–A}} \sum_{q'} e_{q'} (\bar{q}'_\beta q'_\alpha)_{\text{V+A}} \\ Q_9^r = \frac{3}{2} (\bar{r}_\alpha b_\alpha)_{\text{V–A}} \sum_{q'} e_{q'} (\bar{q}'_\beta q'_\beta)_{\text{V–A}} \\ Q_{10}^r = \frac{3}{2} (\bar{r}_\alpha b_\beta)_{\text{V–A}} \sum_{q'} e_{q'} (\bar{q}'_\beta q'_\alpha)_{\text{V–A}}. \end{array} \tag{32}$$

At a renormalization scale $\mu = O(m_b)$, the Wilson coefficients of the current–current operators are $C_1(\mu) = O(10^{-1})$ and $C_2(\mu) = O(1)$, whereas those of the penguin operators are as large as $O(10^{-2})$.[34]

The short-distance part of (29) is nowadays under full control. On the other hand, the long-distance piece suffers still from large theoretical uncertainties. For a given non-leptonic decay $\bar{B} \to \bar{f}$, it is given by the hadronic matrix elements $\langle \bar{f} | Q_k(\mu) | \bar{B} \rangle$ of the four-quark operators. A popular way of dealing with these quantities is to assume that they "factorize" into the product of the matrix elements of two quark currents at some "factorization scale" $\mu = \mu_{\text{F}}$. This procedure can be justified in the large-N_{C} approximation,[36] where N_{C} is the number of $SU(N_{\text{C}})$ quark colours, and there are decays, where this concept can be justified because of "colour transparency" arguments.[37] However, it is in general not on solid ground.

Interesting theoretical progress could be made through the development of the "QCD factorization" (QCDF)[38] and "perturbative QCD" (PQCD)[39] approaches, the soft collinear effective theory (SCET),[40] and QCD light-cone sum-rule methods.[41] An important target of these methods is given by $B \to \pi\pi$ and $B \to \pi K$ decays. Thanks to the B factories, the corresponding theoretical results can now be confronted with experiment. Since the data indicate large non-factorizable corrections,[30,42–45] the long-distance contributions to these decays remain a theoretical challenge.

3.4. *Towards the Exploration of CP Violation*

3.4.1. *Direct CP Violation*

Let us now have a closer look at the amplitude structure of non-leptonic B decays. Because of the unitarity of the CKM matrix, at most two weak amplitudes contribute to such modes in the SM. Consequently, the corresponding transition amplitudes can be written as follows:

$$A(\bar{B} \to \bar{f}) = e^{+i\varphi_1}|A_1|e^{i\delta_1} + e^{+i\varphi_2}|A_2|e^{i\delta_2} \tag{33}$$

$$A(B \to f) = e^{-i\varphi_1}|A_1|e^{i\delta_1} + e^{-i\varphi_2}|A_2|e^{i\delta_2}. \tag{34}$$

Here the $\varphi_{1,2}$ denote CP-violating weak phases, originating from the CKM matrix, whereas the $|A_{1,2}|e^{i\delta_{1,2}}$ are CP-conserving "strong" amplitudes, which contain the whole hadron dynamics of the decay at hand:

$$|A_j|e^{i\delta_j} \sim \sum_k C_k(\mu)\langle \bar{f}|Q_k^j(\mu)|\bar{B}\rangle. \tag{35}$$

Using (33) and (34), we obtain the following CP asymmetry:

$$\begin{aligned} A_{\rm CP} &\equiv \frac{\Gamma(B \to f) - \Gamma(\bar{B} \to \bar{f})}{\Gamma(B \to f) + \Gamma(\bar{B} \to \bar{f})} = \frac{|A(B \to f)|^2 - |A(\bar{B} \to \bar{f})|^2}{|A(B \to f)|^2 + |A(\bar{B} \to \bar{f})|^2} \\ &= \frac{2|A_1||A_2|\sin(\delta_1 - \delta_2)\sin(\varphi_1 - \varphi_2)}{|A_1|^2 + 2|A_1||A_2|\cos(\delta_1 - \delta_2)\cos(\varphi_1 - \varphi_2) + |A_2|^2}. \end{aligned} \tag{36}$$

We observe that a non-vanishing value can be generated through the interference between the two weak amplitudes, provided both a non-trivial weak phase difference $\varphi_1 - \varphi_2$ and a non-trivial strong phase difference $\delta_1 - \delta_2$ are present. This kind of CP violation is referred to as "direct" CP violation, as it originates directly at the amplitude level of the considered decay. It is the B-meson counterpart of the effect that is probed through $\mathrm{Re}(\varepsilon'/\varepsilon)$ in

the neutral kaon system,[a] and could recently be established with the help of $B_d \to \pi^{\mp} K^{\pm}$ decays,[8] as we will see in Subsection 8.3.2.

3.4.2. *Strategies*

Since $\varphi_1 - \varphi_2$ is in general given by one of the angles of the UT – usually γ – the goal is to extract this quantity from the measured value of $A_{\rm CP}$. Unfortunately, hadronic uncertainties enter this game through the poorly known hadronic matrix elements in (35). In order to deal with this problem, we may proceed along one of the following two avenues:

(i) Amplitude relations can be used to eliminate the hadronic matrix elements. We distinguish between exact relations, using pure "tree" decays of the kind $B \to KD$ or $B_c \to D_s D$, and relations, which follow from the flavour symmetries of strong interactions, i.e. isospin or $SU(3)_{\rm F}$, and involve $B_{(s)} \to \pi\pi, \pi K, KK$ modes.

(ii) In decays of neutral B_q mesons ($q \in \{d, s\}$), interference effects between B_q^0–$\bar{B}_q^0$ mixing and decay processes may induce "mixing-induced CP violation". If a single CKM amplitude governs the decay, the hadronic matrix elements cancel in the corresponding CP asymmeties; otherwise we have to use again amplitude relations.

3.4.3. *CP Violation in Neutral B_q Decays*

Since neutral B_q mesons are a key element for the exploration of CP violation, let us next have a closer look at their most important features. A particularly simple – but also very interesting – situation arises in decays into final states f that are eigenstates of the CP operator, i.e. satisfy

$$\hat{C}\hat{P}|f\rangle = \pm|f\rangle. \tag{37}$$

If we solve the Schrödinger equation describing B_q^0–$\bar{B}_q^0$ mixing as we noted in Subsection 3.1, we obtain the following time-dependent CP asymmetry:

$$\left.\frac{\Gamma(B_q^0(t) \to f) - \Gamma(\bar{B}_q^0(t) \to f)}{\Gamma(B_q^0(t) \to f) + \Gamma(\bar{B}_q^0(t) \to f)}\right|_{\Delta\Gamma_q = 0} = A_{\rm CP}^{\rm dir}(B_q \to f)\,\cos(\Delta M_q t) + A_{\rm CP}^{\rm mix}(B_q \to f)\,\sin(\Delta M_q t). \tag{38}$$

[a] For the calculation of $\mathrm{Re}(\varepsilon'/\varepsilon)$, an approriate low-energy effective Hamiltonian with the same structure as (29) is used. The large theoretical uncertainties mentioned after (1) originate from a strong cancellation between the QCD and EW penguin contributions (caused by the large top-quark mass), and the associated hadronic matrix elements.

Here the coefficient of the $\cos(\Delta M_q t)$ term is given by

$$A_{\rm CP}^{\rm dir}(B_q \to f) = \frac{|A(B_q^0 \to f)|^2 - |A(\bar{B}_q^0 \to \bar{f})|^2}{|A(B_q^0 \to f)|^2 + |A(\bar{B}_q^0 \to \bar{f})|^2}, \tag{39}$$

and measures the direct CP violation in the decay $B_q \to f$. As we have seen in (36), this phenomenon originates from the interference between different weak amplitudes. On the other hand, the coefficient of the $\sin(\Delta M_q t)$ term describes another kind of CP violation, which is caused by the interference between B_q^0–$\bar{B}_q^0$ mixing and decay processes, and is referred to as "mixing-induced" CP violation. Mathematically, it is described by

$$A_{\rm CP}^{\rm mix}(B_q \to f) \equiv \frac{2\,{\rm Im}\,\xi_f^{(q)}}{1 + \left|\xi_f^{(q)}\right|^2}, \tag{40}$$

where

$$\xi_f^{(q)} = \pm e^{-i\Theta_{\rm M}^{(q)}} \left[\frac{A(\bar{B}_q^0 \to \bar{f})}{A(B_q^0 \to f)}\right] \tag{41}$$

involves the CP-violating weak phase $\Theta_{\rm M}^{(q)}$ that is associated with B_q^0–$\bar{B}_q^0$ mixing. In the SM, it is related to the CKM phase of the box diagrams with internal top-quark exchanges shown in Fig. 3 as follows:

$$\Theta_{\rm M}^{(q)} - \pi = 2\arg(V_{tq}^* V_{tb}) \equiv \phi_q = \begin{cases} +2\beta = O(47^\circ) & (q = d) \\ -2\delta\gamma = O(-1^\circ) & (q = s), \end{cases} \tag{42}$$

where β and $\delta\gamma$ were introduced in Figs. 1 (a) and (b), respectively.

If we use (33) and (34), we may rewrite (41) as follows:

$$\xi_f^{(q)} = \mp\, e^{-i\phi_q} \left[\frac{e^{+i\varphi_1}|A_1|e^{i\delta_1} + e^{+i\varphi_2}|A_2|e^{i\delta_2}}{e^{-i\varphi_1}|A_1|e^{i\delta_1} + e^{-i\varphi_2}|A_2|e^{i\delta_2}}\right], \tag{43}$$

and observe – in analogy to the discussion of direct CP violation in 3.4.1 – that this quantity suffers, in general, also from large hadronic uncertainties. However, if one CKM amplitude plays the dominant rôle, we arrive at

$$\xi_f^{(q)} = \mp\, e^{-i\phi_q} \left[\frac{e^{+i\phi_f/2}|M_f|e^{i\delta_f}}{e^{-i\phi_f/2}|M_f|e^{i\delta_f}}\right] = \mp\, e^{-i(\phi_q - \phi_f)}. \tag{44}$$

Consequently, the hadronic matrix element $|M_f|e^{i\delta_f}$ cancels in this special case. Since the requirements for direct CP violation are obviously no longer satisfied, the observable $A_{\rm CP}^{\rm dir}(B_q \to f)$ vanishes. On the other hand, we may still have mixing-induced CP violation. In particular,

$$A_{\rm CP}^{\rm mix}(B_q \to f) = \pm \sin\phi \tag{45}$$

is now governed by the CP-violating weak phase difference $\phi \equiv \phi_q - \phi_f$ and is *not* affected by hadronic uncertainties. The corresponding time-dependent CP asymmetry takes then the simple form

$$\left.\frac{\Gamma(B_q^0(t) \to f) - \Gamma(\bar{B}_q^0(t) \to \bar{f})}{\Gamma(B_q^0(t) \to f) + \Gamma(\bar{B}_q^0(t) \to \bar{f})}\right|_{\Delta\Gamma_q=0} = \pm \sin\phi \, \sin(\Delta M_q t), \qquad (46)$$

and allows an elegant determination of $\sin\phi$. In Sections 6 and 7, we will see that this formalism has powerful applications for the search of NP.

4. Rare Decays

4.1. *General Features*

The exploration of flavour physics through CP violation can nicely be complemented through "rare" decays. In the SM, these processes do *not* arise at the tree level, but can originate through *loop* effects. Consequently, rare B decays are mediated by FCNC processes of the kind $\bar{b} \to \bar{s}$ or $\bar{b} \to \bar{d}$, whereas rare K decays originate from their $\bar{s} \to \bar{d}$ counterparts. Prominent examples of rare B decays are the following exclusive channels:

- $B \to K^*\gamma$, $B \to \rho\gamma$, ...
- $B \to K^*\mu^+\mu^-$, $B \to \rho\mu^+\mu^-$, ...
- $B_{s,d} \to \mu^+\mu^-$.

While the $B_{s,d} \to \mu^+\mu^-$ transitions are very clean, the former two decay classes suffer from theoretical uncertainties that are related to hadronic form factors and long-distance contributions. On the other hand, the hadronic uncertainties are much smaller in the corresponding inclusive decays, $B \to X_{s,d}\gamma$ and $B \to X_{s,d}\mu^+\mu^-$, which are therefore more promising from the theoretical point of view, but are unfortunately more difficult to measure; the cleanest rare B decays are given by $B \to X_{s,d}\nu\bar{\nu}$ processes. A tremendous amount of work went into the calculation of the branching ratio of the prominent $B \to X_s\gamma$ decay,[46] and the agreement of the experimental value with the SM expectation implies important constraints for the allowed parameter space of popular NP scenarios. The phenomenology of the kaon system includes also interesting rare decays:[16,29]

- $K_{\rm L} \to \pi^0 e^+ e^-$, $K_{\rm L} \to \pi^0 \mu^+ \mu^-$
- $K_{\rm L} \to \pi^0 \nu\bar{\nu}$, $K^+ \to \pi^+ \nu\bar{\nu}$.

4.2. *Theoretical Description*

For the theoretical description of rare decays, low-energy effective Hamiltonians are used, in analogy to the analysis of non-leptonic B decays. The structure of the corresponding transition amplitudes is therefore similar to the one of (21), i.e. the short-distance physics is described by perturbatively calculable Wilson coefficient functions, whereas the long-distance dynamics is encoded in non-perturbative hadronic matrix elements of local operators. It is useful to rewrite the rare-decay implementation of (21) as follows:[47,48]

$$A(\text{decay}) = P_0(\text{decay}) + \sum_r P_r(\text{decay}) F_r(x_t \equiv m_t^2/M_W^2). \qquad (47)$$

Here $\mu = \mu_0 = O(M_W)$ was chosen, and the Wilson coefficients $C_k(\mu_0)$ were expressed in terms of "master functions" $F_r(x_t)$. These quantities follow from the evaluation of penguin and box diagrams with heavy particles running in the loops, i.e. top and W in the SM, and are related to the Inami–Lim functions.[35] On the other hand, the term P_0 summarizes the contributions from light internal quarks, such as the charm and up quarks. It should be noted that P_0 and P_r are *process-dependent* quantities, i.e. depend on the hadronic matrix elements of the operators Q_k for a given decay, whereas the $F_r(x_t)$ are *process-independent* functions. In Section 5, we will return to this formalism in the context of NP.

Rare decays have many interesting features, as discussed in several reviews and the references therein.[16,34,46,49] Let us here choose $B_{s,d} \to \mu^+\mu^-$ modes as a representative example, since these decays allow a compact presentation, belong to the cleanest representatives of the field of rare decays, and are an important element of the B-physics programme at the LHC.[50]

4.3. *Example:* $B_{s,d} \to \mu^+\mu^-$

In the SM, $B_q \to \mu^+\mu^-$ modes ($q \in \{s, d\}$) originate from Z^0 penguins and box diagrams, as can be seen in Fig. 7. The corresponding low-energy effective Hamiltonian is given as follows:

$$H_{\text{eff}} = -\frac{G_{\text{F}}}{\sqrt{2}} \left[\frac{\alpha}{2\pi \sin^2 \Theta_{\text{W}}}\right] V_{tb}^* V_{tq} \eta_Y Y_0(x_t) (\bar{b}q)_{\text{V-A}} (\bar{\mu}\mu)_{\text{V-A}} + \text{h.c.}, \quad (48)$$

where α denotes the QED coupling, Θ_{W} is the Weinberg angle, and the short-distance physics is described by

$$Y(x_t) \equiv \eta_Y Y_0(x_t). \qquad (49)$$

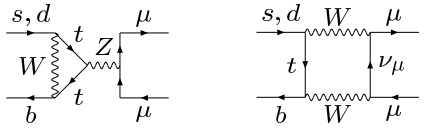

Figure 7. Decay processes contributing to $B_{s,d} \to \mu^+\mu^-$ in the SM.

Here $\eta_Y = 1.012$ is a perturbative QCD correction,[51–53] and the Inami–Lim function $Y_0(x_t)$, which can be written to a good approximation as

$$Y_0(x_t) = 0.98 \times \left[\frac{m_t}{167\,\mathrm{GeV}}\right]^{1.56}, \tag{50}$$

describes the top-quark mass dependence.[54] We observe that the matrix element of (48) between a $\langle\mu^-\mu^+|$ final state and a $|B_q^0\rangle$ initial state involves simply the "decay constant" f_{B_q}, which is defined through[b]

$$\langle 0|\bar{b}\gamma_\alpha\gamma_5 q|B_q^0(k)\rangle = i f_{B_q} k_\alpha. \tag{51}$$

Consequently, we encounter a very favourable situation with respect to the hadronic matrix elements. Since, moreover, NLO QCD corrections were calculated, and long-distance contributions are expected to play a negligible rôle,[51] the $B_q \to \mu^+\mu^-$ modes belong to the cleanest rare B decays.

In the SM, their branching ratios can be written as[55]

$$\begin{aligned}\mathrm{BR}(B_s \to \mu^+\mu^-) &= 4.1 \times 10^{-9} \\ &\times \left[\frac{f_{B_s}}{0.24\,\mathrm{GeV}}\right]^2 \left[\frac{|V_{ts}|}{0.040}\right]^2 \left[\frac{\tau_{B_s}}{1.5\,\mathrm{ps}}\right] \left[\frac{m_t}{167\,\mathrm{GeV}}\right]^{3.12} \qquad (52)\\ \mathrm{BR}(B_d \to \mu^+\mu^-) &= 1.1 \times 10^{-10} \\ &\times \left[\frac{f_{B_d}}{0.20\,\mathrm{GeV}}\right]^2 \left[\frac{|V_{td}|}{0.008}\right]^2 \left[\frac{\tau_{B_d}}{1.5\,\mathrm{ps}}\right] \left[\frac{m_t}{167\,\mathrm{GeV}}\right]^{3.12}, \qquad (53)\end{aligned}$$

which should be compared with the current experimental upper bounds:

$$\mathrm{BR}(B_s \to \mu^+\mu^-) < 5.0 \times 10^{-7}\ [\text{D0 @ 95\% C.L.}^{56}] \tag{54}$$

$$\mathrm{BR}(B_d \to \mu^+\mu^-) < 8.3 \times 10^{-8}\ [\text{BaBar @ 90\% C.L.}^{57}]. \tag{55}$$

If we use the relation

$$R_t \equiv \frac{1}{\lambda}\left|\frac{V_{td}}{V_{cb}}\right| = \frac{1}{\lambda}\left|\frac{V_{td}}{V_{ts}}\right|\left[1 + O(\lambda^2)\right], \tag{56}$$

[b] Note that $\langle 0|\bar{b}\gamma_\alpha q|B_q^0(k)\rangle = 0$, since the B_q^0 is a pseudoscalar meson.

we observe that the measurement of the ratio

$$\frac{\mathrm{BR}(B_d \to \mu^+\mu^-)}{\mathrm{BR}(B_s \to \mu^+\mu^-)} = \left[\frac{\tau_{B_d}}{\tau_{B_s}}\right] \left[\frac{M_{B_d}}{M_{B_s}}\right] \left[\frac{f_{B_d}}{f_{B_s}}\right]^2 \left|\frac{V_{td}}{V_{ts}}\right|^2 \tag{57}$$

would allow a determination of the UT side R_t. This strategy is complementary to the one addressed in Subsection 2.5, which is offered by

$$\frac{\Delta M_d}{\Delta M_s} = \left[\frac{M_{B_d}}{M_{B_s}}\right] \left[\frac{\hat{B}_{B_d}}{\hat{B}_{B_s}}\right] \left[\frac{f_{B_d}}{f_{B_s}}\right]^2 \left|\frac{V_{td}}{V_{ts}}\right|^2, \tag{58}$$

where the $\hat{B}_{B_q}$ are non-perturbative "bag" parameters arising in B^0_q–$\bar{B}^0_q$ mixing. These determinations rely on the following $SU(3)$-breaking ratios:

$$\frac{f_{B_s}}{f_{B_d}}, \quad \xi \equiv \frac{\sqrt{\hat{B}_s} f_{B_s}}{\sqrt{\hat{B}_d} f_{B_d}}, \tag{59}$$

which can be obtained from QCD lattice studies or with the help of QCD sum rules, and are an important target of current research.[58] Looking at (57) and (58), we see that these expressions imply the relation

$$\frac{\mathrm{BR}(B_s \to \mu^+\mu^-)}{\mathrm{BR}(B_d \to \mu^+\mu^-)} = \left[\frac{\tau_{B_s}}{\tau_{B_d}}\right] \left[\frac{\hat{B}_{B_d}}{\hat{B}_{B_s}}\right] \left[\frac{\Delta M_s}{\Delta M_d}\right], \tag{60}$$

which suffers from theoretical uncertainties that are smaller than those affecting (57) and (58) since the dependence on $(f_{B_d}/f_{B_s})^2$ cancels and $\hat{B}_{B_d}/\hat{B}_{B_s} = 1$ up to tiny $SU(3)$-breaking corrections.[59] Moreover, we may also use the (future) experimental data for $\Delta M_{(s)d}$ to reduce the hadronic uncertainties of the SM predictions of the $B_q \to \mu^+\mu^-$ branching ratios:

$$\mathrm{BR}(B_s \to \mu^+\mu^-) = (3.42 \pm 0.53) \times \left[\frac{\Delta M_s}{18.0\,\mathrm{ps}^{-1}}\right] \times 10^{-9} \tag{61}$$

$$\mathrm{BR}(B_d \to \mu^+\mu^-) = (1.00 \pm 0.14) \times 10^{-10}. \tag{62}$$

In view of these tiny branching ratios, we could only hope to observe the $B_q \to \mu^+\mu^-$ decays at the LHC, should they actually be governed by their SM contributions.[50] However, as these transitions are mediated by rare FCNC processes, they are sensitive probes of NP. In particular, as was recently reviewed,[15] the $B_q \to \mu^+\mu^-$ branching ratios may be dramatically enhanced in specific NP (SUSY) scenarios. Should this actually be the case, these decays may be seen at run II of the Tevatron, and the e^+e^- B factories could observe $B_d \to \mu^+\mu^-$.

The interpretation of the present and future experimental constraints on $B_s \to \mu^+\mu^-$ in the context of the constrained minimal extension of the SM (CMSSM) with universal scalar masses was recently critically discussed.[60]

5. How Could New Physics Enter?

5.1. *Twofold Impact of New Physics*

In order to address the question of how NP affects flavour physics, we use once agian the language of the low-energy effective Hamiltonians introduced above. There are then two possibilities for NP to manifest itself:[15]

(i) NP may modify the "strength" of the operators arising in the SM. In this case, we obtain new short-distance functions that depend on the NP parameters, such as masses of charginos, squarks, charged Higgs particles and $\tan\bar{\beta} \equiv v_2/v_1$ in the MSSM. The NP particles enter in new box and penguin diagrams and are "integrated out" as the W and top, so that we arrive at initial conditions for the renormalization-group evolution (26) of the following structure:

$$C_k(\mu = M_W) \to C_k^{\rm SM} + C_k^{\rm NP}, \tag{63}$$

where the NP pieces $C_k^{\rm NP}$ may also involve new CP-violating phases that are *not* related to the CKM matrix.

(ii) NP may lead to an enlarged operator basis:

$$\{Q_k\} \to \{Q_k^{\rm SM}, Q_l^{\rm NP}\}, \tag{64}$$

i.e. operators that are absent (or strongly suppressed) in the SM may actually play an important rôle, thereby yielding, in general, also new sources for flavour and CP violation.

5.2. *Classification of New Physics*

After these general considerations, NP can be divided into the following classes, as was done by Buras:[15]

Class A: this class describes models with "minimal flavour violation" (MFV), which represent the simplest extension of the SM. Here the flavour-changing processes are still governed by the CKM matrix – in particular there are no new sources for CP violation – and the only relevant operators are those present in the SM. If we use v as an abbreviation for the set of parameters involved, the $F_r(x_t)$ introduced in (47) are simply replaced by generalized functions $F_r(v)$, which involve only seven "master functions", $S(v)$, $X(v)$, $Y(v)$, $Z(v)$, $E(v)$, $D'(v)$, $E'(v)$. In (48), we encountered already one of them, the function Y, which characterizes rare K, B decays with $\ell^+\ell^-$ in the final states. Concerning $B_q \to \mu^+\mu^-$ decays, the NP effects can hence be included through the simple replacement $Y(x_t) \to Y(v)$.

A similar procedure applies to the expressions for ΔM_q, where a function $S(v)$ is involved. Since the *same* functions enter in the B_s- and B_d-meson cases, relations (57), (58) and (60) hold not only in the SM, but also in the whole class of MFV models, thereby providing an interesting test of this NP scenario. Examples are the THDM-II and constrained MSSM if $\tan\bar{\beta}$ is not too large, as well as models with one extra universal dimension.

Class B: in contrast to class A, new operators arise, but still no new CP-violating phases are present. Examples of new Dirac structures are $(\mathrm{V}-\mathrm{A})\otimes(\mathrm{V}+\mathrm{A})$, $(\mathrm{S}-\mathrm{P})\otimes(\mathrm{S}\pm\mathrm{P})$, $\sigma_{\mu\nu}(\mathrm{S}-\mathrm{P})\otimes\sigma^{\mu\nu}(\mathrm{S}-\mathrm{P})$, which become relevant for B^0_q–$\bar{B}^0_q$ mixing in the MSSM with large $\tan\bar{\beta}$.

Class C: in contrast to class A, the Wilson coefficients of the usual SM operators may acquire new CP-violating phases, i.e. the C_k^{NP} in (63) may become complex, whereas new operators give still negligible contributions. An example is the MSSM with a value of $\tan\bar{\beta}$ that is not too large and with non-diagonal elements in the squark mass matrices.

Class D: this class describes the general case of physics beyond the SM with new operators *and* new CP-violating phases, and is therefore very involved. Examples are multi-Higgs models with complex phases in the Higgs sector, general SUSY scenarios, models with spontaneous CP violation and left–right-symmetric models.

Class E: in contrast to the classes introduced above, the three-generation CKM matrix is now *not unitary*, so that the UT does not close. An example is given by models with four generations.

5.3. *Impact on the Roadmap of Quark-Flavour Physics*

The B-meson system offers a variety of processes and strategies for the exploration of CP violation.[61] Looking at Fig. 8, where we have collected prominent examples, we see that there are processes with a very *different* dynamics that are – within the framework of the SM – sensitive to the *same* angles of the UT. Moreover, rare B- and K-meson decays, which originate from loop effects in the SM, provide complementary insights into flavour physics and interesting correlations with the CP-B sector.

In the presence of NP, the subtle interplay between different processes is expected to be disturbed, so that discrepancies should emerge. There are two popular avenues for NP to enter the roadmap of flavour physics:

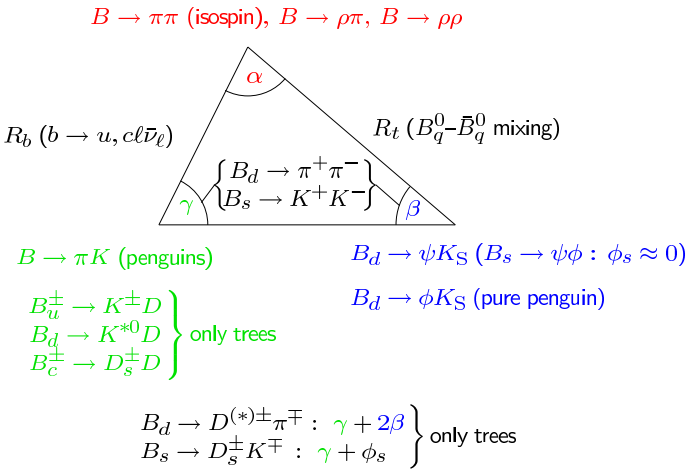

Figure 8. A brief roadmap of B-decay strategies for the exploration of CP violation.

(i) B_q^0–$\bar{B}_q^0$ *mixing:* NP may enter through the exchange of new particles in the box diagrams, or through new contributions at the tree level, thereby modifying the mixing parameters as follows:

$$\Delta M_q = \Delta M_q^{\rm SM} + \Delta M_q^{\rm NP}, \quad \phi_q = \phi_q^{\rm SM} + \phi_q^{\rm NP}. \tag{65}$$

Whereas $\Delta M_q^{\rm NP}$ would affect the determination of the UT side R_t, the NP contribution $\phi_q^{\rm NP}$ would enter the mixing-induced CP asymmetries. Using dimensional arguments borrowed from effective field theory,[62,63] it can be shown that $\Delta M_q^{\rm NP}/\Delta M_q^{\rm SM} \sim 1$ and $\phi_q^{\rm NP}/\phi_q^{\rm SM} \sim 1$ may – in principle – be possible for a NP scale $\Lambda_{\rm NP}$ in the TeV regime; such a pattern may also arise in specific NP scenarios. However, thanks to the B-factory data, the space for NP is getting smaller and smaller in the B_d-meson system. On the other hand, the B_s sector is still essentially unexplored, and leaves a lot of hope for the LHC era. In Section 6, we will discuss the corresponding "golden" decays, $B_d \to J/\psi K_S$ and $B_s \to J/\psi\phi$.

(ii) *Decay amplitudes:* NP has typically a small effect if SM tree processes play the dominant rôle, as in $B_d \to J/\psi K_S$ decays. On the other hand, there are potentially large effects in the FCNC sector. For instance, new particles may enter in penguin diagrams, or we may encounter new FCNC contributions at the tree level. Sizeable contributions may arise generically in field-theoretical estimates

with $\Lambda_{\rm NP} \sim$ TeV,[64] as well as in specific NP models. Interestingly, there are hints in the current B-factory data that this may actually be the case. In particular, Belle results for the $B_d \to \phi K_{\rm S}$ channel raise the question of whether $(\sin 2\beta)_{\phi K_{\rm S}} = (\sin 2\beta)_{\psi K_{\rm S}}$, and the branching ratios of certain $B \to \pi K$ decays show a puzzling pattern which may indicate NP in the EW penguin sector. These hot topics will be discussed in Sections 7 and 8, respectively.

Let us emphasize that also the D-meson system provides interesting probes for the search of NP:[22] D^0–$\bar{D}^0$ mixing and CP-violating effects are tiny in the SM, but may be enhanced through NP.

Concerning model-dependent NP analyses, in particular SUSY scenarios have received a lot of attention; for a selection of recent studies, see Refs. 65–70. Examples of other fashionable NP scenarios are left–right-symmetric models,[71] scenarios with extra dimensions,[72] models with an extra Z',[73] little Higgs scenarios,[74] and models with a fourth generation.[75]

6. "Golden" Decays of B Mesons

Let us now have a closer look at $B_d \to J/\psi K_{\rm S}$ and $B_s \to J/\psi\phi$, which are important applications of the formalism discussed in Subsection 3.4.3.

6.1. $B_d \to J/\psi K_{\rm S}$

6.1.1. *Amplitude Structure and CP-Violating Observables*

This decay has a CP-odd final state, and originates from $\bar{b} \to \bar{c}c\bar{s}$ quark-level transitions. Consequently, as we have seen in the classification of Subsection 3.2, we have to deal both with tree and with penguin topologies, so that the decay amplitude takes the following form:[76]

$$A(B_d^0 \to J/\psi K_{\rm S}) = \lambda_c^{(s)} \left(A_{\rm T}^{c'} + A_{\rm P}^{c'}\right) + \lambda_u^{(s)} A_{\rm P}^{u'} + \lambda_t^{(s)} A_{\rm P}^{t'}. \qquad (66)$$

In this expression, the

$$\lambda_q^{(s)} \equiv V_{qs} V_{qb}^* \qquad (67)$$

are CKM factors, $A_{\rm T}^{c'}$ is the CP-conserving strong tree amplitude, while the $A_{\rm P}^{q'}$ describe the penguin topologies with internal q-quark exchanges ($q \in \{u, c, t\}$), including QCD and EW penguins; the primes remind us that we are dealing with a $\bar{b} \to \bar{s}$ transition. If we eliminate now $\lambda_t^{(s)}$ with the help of (28) and apply the Wolfenstein parametrization, we arrive at

$$A(B_d^0 \to J/\psi K_{\rm S}) \propto \left[1 + \lambda^2 a e^{i\theta} e^{i\gamma}\right], \qquad (68)$$

where

$$ae^{i\vartheta} \equiv \left(\frac{R_b}{1-\lambda^2}\right)\left[\frac{A_{\rm P}^{u'} - A_{\rm P}^{t'}}{A_{\rm T}^{c'} + A_{\rm P}^{c'} - A_{\rm P}^{t'}}\right] \tag{69}$$

is a hadronic parameter.

Using now the formalism of Subsection 3.4.3 we obtain

$$\xi_{\psi K_{\rm S}}^{(d)} = +e^{-i\phi_d}\left[\frac{1+\lambda^2 ae^{i\vartheta}e^{-i\gamma}}{1+\lambda^2 ae^{i\vartheta}e^{+i\gamma}}\right]. \tag{70}$$

Unfortunately, $ae^{i\vartheta}$, which is a measure for the ratio of the $B_d^0 \to J/\psi K_{\rm S}$ penguin to tree contributions, can only be estimated with large hadronic uncertainties. However, since this parameter enters (70) in a doubly Cabibbo-suppressed way, its impact on the CP-violating observables is practically negligible. We can put this important statement on a more quantitative basis by making the plausible assumption that $a = O(\bar{\lambda}) = O(0.2) = O(\lambda)$, where $\bar{\lambda}$ is a "generic" expansion parameter:

$$A_{\rm CP}^{\rm dir}(B_d \to J/\psi K_{\rm S}) = 0 + O(\overline{\lambda}^3) \tag{71}$$

$$A_{\rm CP}^{\rm mix}(B_d \to J/\psi K_{\rm S}) = -\sin\phi_d + O(\overline{\lambda}^3) \stackrel{\rm SM}{=} -\sin 2\beta + O(\overline{\lambda}^3). \tag{72}$$

Consequently, (72) allows an essentially *clean* determination of $\sin 2\beta$.[7]

6.1.2. *Experimental Status*

Since the CKM fits performed within the SM pointed to a large value of $\sin 2\beta$, $B_d \to J/\psi K_{\rm S}$ offered the exciting perspective of *large* mixing-induced CP violation. In 2001, the measurement of $A_{\rm CP}^{\rm mix}(B_d \to J/\psi K_{\rm S})$ allowed indeed the first observation of CP violation *outside* the K-meson system.[6] The most recent data are still not showing any signal for *direct* CP violation in $B_d \to J/\psi K_{\rm S}$ decays, as is expected from (71), but yield

$$\sin 2\beta = \begin{cases} 0.722 \pm 0.040 \pm 0.023 \ (\text{BaBar}^{77}) \\ 0.728 \pm 0.056 \pm 0.023 \ (\text{Belle}^{78}), \end{cases} \tag{73}$$

which gives the following world average:[79]

$$\sin 2\beta = 0.725 \pm 0.037. \tag{74}$$

The theoretical uncertainties are below the 0.01 level (a recent analysis finds even smaller effects[80]), and can be controlled in the LHC era with the help of the $B_s \to J/\psi K_{\rm S}$ channel.[76]

6.1.3. *What about New Physics?*

The agreement of (74) with the CKM fits is excellent.[31] However, despite this remarkable feature, NP could – in principle – still be hiding in the mixing-induced CP violation observed in $B_d \to J/\psi K_{\rm S}$. The point is that the key quantity is actually the B^0_d–$\bar{B}^0_d$ mixing phase

$$\phi_d = \phi_d^{\rm SM} + \phi_d^{\rm NP} = 2\beta + \phi_d^{\rm NP}, \tag{75}$$

where the world average (74) implies

$$\phi_d = (46.5^{+3.2}_{-3.0})^\circ \quad \vee \quad (133.5^{+3.0}_{-3.2})^\circ. \tag{76}$$

Here the former solution would be in excellent agreement with the CKM fits, yielding $40^\circ \lesssim 2\beta \lesssim 50^\circ$, whereas the latter would correspond to NP.[63,81] Both solutions can be distinguished through the measurement of the sign of $\cos\phi_d$, where a positive value would select the SM case. Performing an angular analysis of $B_d \to J/\psi[\to \ell^+\ell^-]K^*[\to \pi^0 K_{\rm S}]$ processes, the BaBar collaboration finds[82]

$$\cos\phi_d = 2.72^{+0.50}_{-0.79} \pm 0.27, \tag{77}$$

thereby favouring the SM. Interestingly, this picture emerges also from the first data for CP-violating effects in $B_d \to D^{(*)\pm}\pi^\mp$ modes,[83] and an analysis of $B \to \pi\pi, \pi K$ decays,[42] although in an indirect manner.

As far as NP contributions at the amplitude level are concerned, they have to compete with SM tree-diagram-like topologies, which play the dominant rôle in the $B \to J/\psi K$ modes. Consequently, the NP contributions to the decay amplitudes are generically at most at the 10% level; these effects could be detected through appropriate observables, exploiting direct CP violation and charged $B^\pm \to J/\psi K^\pm$ decays.[62] Since the current B-factory data do not give any indication for NP of this kind, we eventually arrive at the situation in the $\bar{\rho}$–$\bar{\eta}$ plane shown in Fig. 2. The space for NP contributions to B^0_d–$\bar{B}^0_d$ mixing is therefore getting smaller and smaller. However, there is still hope for NP effects in B^0_s–$\bar{B}^0_s$ mixing, which can nicely be probed through $B_s \to J/\psi\phi$, the B_s-meson counterpart of $B_d \to J/\psi K_{\rm S}$.

6.2. $B_s \to J/\psi\phi$

6.2.1. *Preliminaries: Characteristic Features of B^0_s–$\bar{B}^0_s$ Mixing*

At the e^+e^- B factories operating at the $\Upsilon(4S)$ resonance, *no* B_s mesons are accessible, whereas we obtain plenty of B_s mesons at hadron colliders, i.e. at Tevatron-II and the LHC. The B_s system has interesting features:

- In the SM, the B_s^0–$\bar{B}_s^0$ oscillations are expected to be much faster than their B_d-meson counterparts, and could so far not be observed. The current lower bound for the mass difference of the B_s mass eigenstates is given as follows:[79]

$$\Delta M_s|_{\rm SM} > 14.4\,{\rm ps}^{-1}\ (95\%\ {\rm C.L.}), \tag{78}$$

  and plays an important rôle in the CKM fits.[58]
- In contrast to the B_d-meson system, the width difference $\Delta\Gamma_s$ is expected to be sizable in the B_s case,[84] and may therefore allow interesting studies with the following "untagged" B_s rates:[85,86]

$$\langle\Gamma(B_q(t)\to f)\rangle \equiv \Gamma(B_q^0(t)\to f) + \Gamma(\bar{B}_q^0(t)\to f). \tag{79}$$

  Recently, the first results for $\Delta\Gamma_s$ were reported from the Tevatron, using the $B_s\to J/\psi\phi$ channel:[87]

$$\frac{|\Delta\Gamma_s|}{\Gamma_s} = \begin{cases} 0.65^{+0.25}_{-0.33} \pm 0.01 & ({\rm CDF}^{88}) \\ 0.21^{+0.33}_{-0.45} & ({\rm D0}^{89}). \end{cases} \tag{80}$$

- Finally, let us emphasize again that ϕ_s is negligibly small in the SM, whereas ϕ_d takes the large value of $2\beta = (46.5^{+3.2}_{-3.0})^\circ$.

6.2.2. *CP Violation in $B_s\to J/\psi\phi$*

This channel is simply related to $B_d\to J/\psi K_{\rm S}$ through a replacement of the down spectator quark by a strange quark. Consequently, the structure of the $B_s\to J/\psi\phi$ decay amplitude is completely analogous to (68). On the other hand, the final state of $B_s\to J/\psi\phi$ is an admixture of different CP eigenstates, which can, however, be disentangled through an angular analysis.[87,90] The corresponding angular distribution exhibits tiny direct CP violation, and allows the extraction of

$$\sin\phi_s + O(\overline{\lambda}^3) = \sin\phi_s + O(10^{-3}) \tag{81}$$

through mixing-induced CP violation. Since $\phi_s = -2\lambda^2\eta = O(10^{-2})$ in the SM, the determination of this phase from (81) is affected by hadronic uncertainties of $O(10\%)$, which may become an important issue for the LHC era. These uncertainties can be controlled with the help of flavour-symmetry arguments through the decay $B_d\to J/\psi\rho^0$.[91]

Because of its nice experimental signature, $B_s\to J/\psi\phi$ is very accessible at hadron colliders, and can be fully exploited at the LHC. Needless to note, the big hope is that *sizeable* CP violation will be found in this channel. Since the CP-violating effects in $B_s\to J/\psi\phi$ are tiny in the SM, this would give us

an unambiguous signal for NP.[92] As the situation for NP entering through the decay amplitude is similar to $B \to J/\psi K$, we would get immediate evidence for NP contributions to B_s^0–$\bar{B}_s^0$ mixing, and could extract the corresponding *sizeable* value of ϕ_s.[93] Such a scenario may generically arise in the presence of NP with $\Lambda_{\rm NP} \sim$ TeV,[61] as well as in specific models (see, e.g., Refs. 66, 68). In such studies, also correlations with CP-violating effects in $B_d \to \phi K_{\rm S}$ are typically investigated, which is our next topic.

7. Challenging the Standard Model through $B_d \to \phi K_{\rm S}$

7.1. *Amplitude Structure and CP-Violating Observables*

Another important probe for the testing of the KM mechanism is offered by $B_d^0 \to \phi K_{\rm S}$, which is a decay into a CP-odd final state, and originates from $\bar{b} \to \bar{s}s\bar{s}$ transitions. Consequently, it is a pure penguin mode, which is dominated by QCD penguins.[94] Because of the large top-quark mass, EW penguins have a sizeable impact as well.[95,96] In the SM, we may write

$$A(B_d^0 \to \phi K_{\rm S}) = \lambda_u^{(s)} \tilde{A}_{\rm P}^{u'} + \lambda_c^{(s)} \tilde{A}_{\rm P}^{c'} + \lambda_t^{(s)} \tilde{A}_{\rm P}^{t'}, \tag{82}$$

where we have applied the same notation as in Subsection 6.1. Eliminating once more the CKM factor $\lambda_t^{(s)}$ with the help of (28) yields

$$A(B_d^0 \to \phi K_{\rm S}) \propto \left[1 + \lambda^2 b e^{i\Theta} e^{i\gamma}\right], \tag{83}$$

where

$$b e^{i\Theta} \equiv \left(\frac{R_b}{1-\lambda^2}\right) \left[\frac{\tilde{A}_{\rm P}^{u'} - \tilde{A}_{\rm P}^{t'}}{\tilde{A}_{\rm P}^{c'} - \tilde{A}_{\rm P}^{t'}}\right]. \tag{84}$$

Consequently, we obtain

$$\xi_{\phi K_{\rm S}}^{(d)} = +e^{-i\phi_d} \left[\frac{1 + \lambda^2 b e^{i\Theta} e^{-i\gamma}}{1 + \lambda^2 b e^{i\Theta} e^{+i\gamma}}\right]. \tag{85}$$

The theoretical estimates of $b e^{i\Theta}$ suffer from large hadronic uncertainties. However, since this parameter enters (85) in a doubly Cabibbo-suppressed way, we obtain the following expressions:[97]

$$A_{\rm CP}^{\rm dir}(B_d \to \phi K_{\rm S}) = 0 + O(\lambda^2) \tag{86}$$

$$A_{\rm CP}^{\rm mix}(B_d \to \phi K_{\rm S}) = -\sin\phi_d + O(\lambda^2), \tag{87}$$

where we made the plausible assumption that $b = O(1)$. On the other hand, the mixing-induced CP asymmetry of $B_d \to J/\psi K_{\rm S}$ measures also $-\sin\phi_d$, as we saw in (72). We arrive therefore at the following relation:[97–100]

$$A_{\rm CP}^{\rm mix}(B_d \to \phi K_{\rm S}) = A_{\rm CP}^{\rm mix}(B_d \to J/\psi K_{\rm S}) + O(\lambda^2), \tag{88}$$

which offers a very interesting test of the SM. Since $B_d \to \phi K_{\rm S}$ is governed by penguin processes in the SM, this decay may well be affected by NP. In fact, if we assume that NP arises generically in the TeV regime, it can be shown through field-theoretical estimates that the NP contributions to $b \to s\bar{s}s$ transitions may well lead to sizeable violations of (88); in order to trace the origin of NP systematically, a combined analysis of the neutral and the charged $B \to \phi K$ modes would be very useful.[64]

7.2. *Experimental Status*

It is interesting to have a brief look at the time evolution of the B-factory data. At the LP '03 conference,[101] the picture was as follows:

$$A_{\rm CP}^{\rm dir}(B_d \to \phi K_{\rm S}) = \begin{cases} -0.38 \pm 0.37 \pm 0.12 \ \text{(BaBar)} \\ +0.15 \pm 0.29 \pm 0.07 \ \text{(Belle)} \end{cases} \tag{89}$$

$$A_{\rm CP}^{\rm mix}(B_d \to \phi K_{\rm S}) = \begin{cases} -0.45 \pm 0.43 \pm 0.07 \ \text{(BaBar)} \\ +0.96 \pm 0.50^{+0.11}_{-0.09} \quad \text{(Belle)}. \end{cases} \tag{90}$$

In the summer of last year, the following situation emerged at ICHEP '04:[102]

$$A_{\rm CP}^{\rm dir}(B_d \to \phi K_{\rm S}) = \begin{cases} +0.00 \pm 0.23 \pm 0.05 \ \text{(BaBar}^{[103]}\text{)} \\ -0.08 \pm 0.22 \pm 0.09 \ \text{(Belle}^{[104]}\text{)} \end{cases} \tag{91}$$

$$\underbrace{A_{\rm CP}^{\rm mix}(B_d \to \phi K_{\rm S})}_{\equiv -(\sin 2\beta)_{\phi K_{\rm S}}} = \begin{cases} -0.50 \pm 0.25^{+0.04}_{-0.07} \quad \text{(BaBar}^{[103]}\text{)} \\ -0.06 \pm 0.33 \pm 0.09 \ \text{(Belle}^{[104]}\text{)}. \end{cases} \tag{92}$$

Because of $-(\sin 2\beta)_{\psi K_{\rm S}} \equiv A_{\rm CP}^{\rm mix}(B_d \to J/\psi K_{\rm S}) = -0.725 \pm 0.037$, the Belle data may indicate a violation of (88) through CP-violating NP contributions to $b \to s\bar{s}s$ transitions, which has already stimulated many speculations about NP effects in the decay $B_d \to \phi K_{\rm S}$.[66,68] However, the new Belle data moved towards the SM, and the BaBar data – though also somewhat on the lower side – are in accordance with the SM. Consequently, it seems too early to get too excited by the possibility of having a violation of the SM relation (88).

It will be very interesting to observe how the B-factory data will evolve, and to monitor also similar modes, such as $B_d \to \eta' K_{\rm S}$. However, it is questionable to perform averages over many decays of this kind to argue for NP in $b \to s$ penguin processes, as is frequently done in the literature. The point is that we encounter different hadronic uncertainties in the SM, and that also NP is generally expected to affect these decays differently.

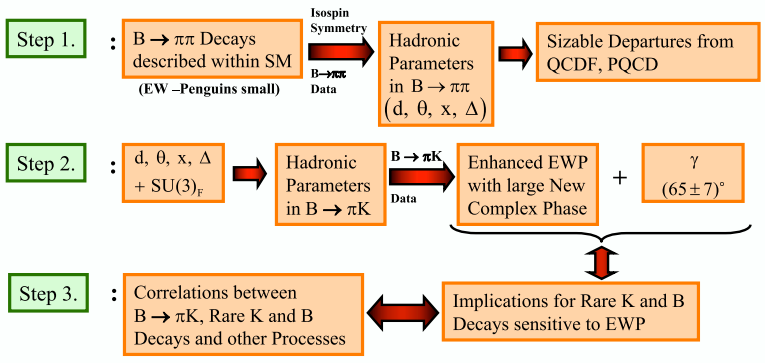

Figure 9. The logical structure of a systematic strategy to analyze the $B \to \pi\pi, \pi K$ puzzles and to explore their implications for rare K and B decays.

8. The $B \to \pi\pi, \pi K$ Puzzles and their Implications for Rare K and B Decays

8.1. *Preliminaries*

For the search of NP signals and the exploration of their specific nature, it is crucial to exploit as much experimental information as possible, and to make also use of the interplay between CP-violating phenomena and rare decays. As an example, let us discuss a strategy, which was recently proposed to analyze puzzling patterns in the data for $B \to \pi\pi$ and $B \to \pi K$ decays, and to investigate their implications for rare K and B decays.[42] Its starting point is the SM, with

$$\phi_d = (46.5^{+3.2}_{-3.0})^\circ \text{ (see (76))}, \quad \gamma = (65 \pm 7)^\circ \text{ (CKM fits)}, \qquad (93)$$

and it consists of three interrelated steps, as illustrated in Fig. 9:

- In step I, we perform an isospin analysis of the currently available $B \to \pi\pi$ data, allowing us to extract a set of hadronic parameters characterizing the $B \to \pi\pi$ system, and to predict the CP-violating $B_d \to \pi^0\pi^0$ observables. We find large non-factorizable effects, but arrive at a picture which is consistent with the SM.
- In step II, we use the hadronic $B \to \pi\pi$ parameters from step I to determine their $B \to \pi K$ counterparts with the help of the $SU(3)$ flavour symmetry, allowing us to predict the $B \to \pi K$ observables in the SM. We find agreement with the B-factory data in the case of those decays that are only marginally affected by EW penguins. Moreover, we may extract γ, in excellent accordance with (93), and can perform a couple of other internal consistency checks, which

also support our working assumptions. On the other hand, in the case of the $B \to \pi K$ decays with a significant impact of EW penguins, we obtain predictions which are *not* in agreement with the current data. This feature is a manifestation of the "$B \to \pi K$ puzzle", which was already pointed out in 2000,[105] and received considerable attention in the recent literature (see, for instance, Refs. 81, 106–110). It can be resolved through NP in the EW penguin sector, which enhances the corresponding contributions and introduces a new CP-violating phase.

- In step III, we assume that NP enters in the EW penguin sector through Z^0 penguins, and explore the interplay of such a scenario with rare K and B decays. Interestingly, spectacular NP effects would arise in several processes, in particular in $K_{\rm L} \to \pi^0 \nu\bar{\nu}$ and $B_{s,d} \to \mu^+\mu^-$ modes, thereby leading to a specific pattern which can be *tested* experimentally.

Let us now have a closer look at these three steps, where the numerical results refer to a recent update.[30]

8.2. *Step I: $B \to \pi\pi$*

8.2.1. *Input Observables*

The $B \to \pi\pi$ system offers three channels, $B^+ \to \pi^+\pi^0$, $B_d^0 \to \pi^+\pi^-$ and $B_d^0 \to \pi^0\pi^0$, as well as their CP conjugates. Consequently, two independent ratios of the corresponding CP-averaged branching ratios are at our disposal, which we may introduce as follows:

$$R_{+-}^{\pi\pi} \equiv 2\left[\frac{{\rm BR}(B^\pm \to \pi^\pm\pi^0)}{{\rm BR}(B_d \to \pi^+\pi^-)}\right]\frac{\tau_{B_d^0}}{\tau_{B^+}} = 2.20 \pm 0.31 \tag{94}$$

$$R_{00}^{\pi\pi} \equiv 2\left[\frac{{\rm BR}(B_d \to \pi^0\pi^0)}{{\rm BR}(B_d \to \pi^+\pi^-)}\right] = 0.67 \pm 0.14. \tag{95}$$

The branching ratios for $B_d \to \pi^+\pi^-$ and $B_d \to \pi^0\pi^0$ are found to be surprisingly small and large, respectively, whereas the one for $B^\pm \to \pi^\pm\pi^0$ is in accordance with theoretical estimates. This feature is reflected by the pattern of $R_{+-}^{\pi\pi} \sim 1.24$ and $R_{00}^{\pi\pi} \sim 0.07$ arising in QCDF.[106] In addition to the CP-conserving observables in (94) and (95), we may also exploit the CP-violating observables of the $B_d \to \pi^+\pi^-$ decay:

$$A_{\rm CP}^{\rm dir}(B_d \to \pi^+\pi^-) = -0.37 \pm 0.11 \tag{96}$$

$$A_{\rm CP}^{\rm mix}(B_d \to \pi^+\pi^-) = +0.61 \pm 0.14. \tag{97}$$

The experimental picture of these CP asymmetries is not yet fully settled.[79] However, their theoretical interpretation discussed below yields constraints for the UT in excellent agreement with the SM.

8.2.2. *Hadronic Parameters*

Using the isospin flavour symmetry of strong interactions, the observables in (94)–(97) depend on two (complex) hadronic parameters, $de^{i\theta}$ and $xe^{i\Delta}$, which describe – sloppily speaking – the ratio of penguin to colour-allowed tree amplitudes and the ratio of colour-suppressed to colour-allowed tree amplitudes, respectively. It is possible to extract these quantities *cleanly* and *unambiguously* from the data:[c]

$$d = 0.51^{+0.26}_{-0.20}, \quad \theta = +(140^{+14}_{-18})^\circ, \quad x = 1.15^{+0.18}_{-0.16}, \quad \Delta = -(59^{+19}_{-26})^\circ; \tag{98}$$

a similar picture is also found by other authors.[43–45] In particular the impressive strong phases give an unambiguous signal for large deviations from "factorization". In recent QCDF[111] and PQCD[112] analyses, the following numbers were obtained:

$$d|_{\rm QCDF} = 0.29 \pm 0.09, \quad \theta|_{\rm QCDF} = -\left(171.4 \pm 14.3\right)^\circ, \tag{99}$$

$$d|_{\rm PQCD} = 0.23^{+0.07}_{-0.05}, \quad +139^\circ < \theta|_{\rm PQCD} < +148^\circ, \tag{100}$$

which depart significantly from the experimental pattern in (98).

8.2.3. *CP Violation in $B_d \to \pi^0\pi^0$*

Having the hadronic paramters of (98) at hand, the CP-violating asymmetries of the $B_d \to \pi^0\pi^0$ channel can be predicted:

$$A_{\rm CP}^{\rm dir}(B_d \to \pi^0\pi^0)\big|_{\rm SM} = -0.28^{+0.37}_{-0.21} \tag{101}$$

$$A_{\rm CP}^{\rm mix}(B_d \to \pi^0\pi^0)\big|_{\rm SM} = -0.63^{+0.45}_{-0.41}, \tag{102}$$

thereby offering the exciting perspective of large CP violation in this decay. The first results for the direct CP asymmetry were recently reported:

$$A_{\rm CP}^{\rm dir}(B_d \to \pi^0\pi^0) = \begin{cases} -(0.12 \pm 0.56 \pm 0.06) & (\text{BaBar}^{113}) \\ -(0.43 \pm 0.51\,^{+0.17}_{-0.16}) & (\text{Belle}^{114}), \end{cases} \tag{103}$$

and correspond to the average of $A_{\rm CP}^{\rm dir}(B_d \to \pi^0\pi^0) = -(0.28 \pm 0.39)$,[79] which shows an encouraging agreement with (101). In the future, more accurate input data will allow us to make much more stringent predictions.

[c] EW penguin topologies have a tiny impact on the $B \to \pi\pi$ system, but are included in the numerical analysis.[30]

8.3. *Step II: $B \to \pi K$*

8.3.1. *Ingredients of the $B \to \pi K$ Analysis*

In contrast to the $B \to \pi\pi$ modes, which originate from $b \to d$ processes, we have to deal with $b \to s$ transitions in the case of the $B \to \pi K$ system. Consequently, these decay classes differ in their CKM structure and exhibit a very different dynamics. In particular, the $B \to \pi K$ decays are dominated by QCD penguins. Concerning the EW penguins, the $B \to \pi K$ decays can be divided as follows:

- $B_d^0 \to \pi^- K^+$, $B^+ \to \pi^+ K^0$ (and CP conjugates): EW penguins are colour-suppressed and expected to play a tiny rôle;
- $B^+ \to \pi^0 K^+$, $B_d^0 \to \pi^0 K^0$ (and CP conjugates): EW penguins are colour-allowed and have therefore a significant impact.

The starting point of our $B \to \pi K$ analysis are the hadronic $B \to \pi\pi$ parameters determined in Subsection 8.2, and the values of ϕ_d and γ in (93), which correspond to the SM and are only insignificantly affected by EW penguins. We use then the following working hypothesis:

(i) $SU(3)$ flavour symmetry of strong interactions;
(ii) neglect of penguin annihilation and exchange topologies.

It is important to stress that internal consistency checks of these assumptions can be performed, which are nicely satisfied by the current data and do not indicate any anomalous behaviour. We may then determine the hadronic $B \to \pi K$ parameters through their $B \to \pi\pi$ counterparts, allowing us to predict the $B \to \pi K$ observables in the SM.

8.3.2. *Observables with a Tiny Impact of EW Penguins*

Let us first have a look at the observables with a *tiny* impact of EW penguins. Here the direct CP asymmetry in $B_d \to \pi^\mp K^\pm$ modes, which could be observed last summer, plays an important rôle. The average of the corresponding BaBar and Belle results[8] is given as follows:[79]

$$A_{\rm CP}^{\rm dir}(B_d \to \pi^\mp K^\pm) = +0.113 \pm 0.01, \tag{104}$$

and establishes direct CP violation in the B-meson system. The non-zero value of this CP asymmetry is generated through the interference between a QCD penguin and a colour-allowed tree amplitude, where the former dominates. In our strategy, we obtain the following prediction:

$$A_{\rm CP}^{\rm dir}(B_d \to \pi^\mp K^\pm) = +0.127^{+0.102}_{-0.066}, \tag{105}$$

which agrees nicely with the experimental value. Moreover, assumptions (i) and (ii) listed in Subsection 8.3.1 imply the following relation:

$$H \propto \underbrace{\left(\frac{f_K}{f_\pi}\right)^2 \left[\frac{\mathrm{BR}(B_d \to \pi^+\pi^-)}{\mathrm{BR}(B_d \to \pi^\mp K^\pm)}\right]}_{0.38\pm0.04} = \underbrace{-\left[\frac{A_{\mathrm{CP}}^{\mathrm{dir}}(B_d \to \pi^\mp K^\pm)}{A_{\mathrm{CP}}^{\mathrm{dir}}(B_d \to \pi^+\pi^-)}\right]}_{0.31\pm0.11}, \quad (106)$$

where we have also indicated the experimental values, which give us further confidence into our working assumptions. Moreover, since we may write

$$H = G_3(d, \theta; \gamma), \quad (107)$$

the $B_d \to \pi^\mp K^\pm$ data allow us to convert the CP asymmetries

$$A_{\mathrm{CP}}^{\mathrm{dir}}(B_d \to \pi^+\pi^-) = G_1(d, \theta; \gamma) \quad (108)$$

$$A_{\mathrm{CP}}^{\mathrm{mix}}(B_d \to \pi^+\pi^-) = G_2(d, \theta; \gamma, \phi_d) \quad (109)$$

into a value of γ.[81,115] The corresponding result is shown as the quadrangle in Fig. 2, which is in excellent agreement with all the other UT constraints.

On the other hand, a moderate numerical discrepancy arises for the ratio R of the CP-averaged $B_d \to \pi^\mp K^\pm$, $B^\pm \to \pi^\pm K$ branching ratios.[116] This feature suggests a sizeable impact of a hadronic parameter $\rho_{\mathrm{c}} e^{i\theta_{\mathrm{c}}}$, which enters the most general parametrization of the $B^+ \to \pi^+ K^0$ amplitude.[117,118] It can be constrained through the direct CP asymmetry of the decay $B^\pm \to \pi^\pm K$ and the emerging $B^\pm \to K^\pm K$ signal, and actually shifts the predicted value of R towards the data.[30] Consequently, no discrepancies with the SM arise in this sector of the $B \to \pi K$ system.

8.3.3. *Observables with a Sizeable Impact of EW Penguins*

Let us now turn to those observables that are significantly affected by EW penguins. The key quantities are the following ratios:[119]

$$R_{\mathrm{c}} \equiv 2\left[\frac{\mathrm{BR}(B^+ \to \pi^0 K^+) + \mathrm{BR}(B^- \to \pi^0 K^-)}{\mathrm{BR}(B^+ \to \pi^+ K^0) + \mathrm{BR}(B^- \to \pi^- \bar{K}^0)}\right] \stackrel{\mathrm{Exp}}{=} 1.00 \pm 0.08 \quad (110)$$

$$R_{\mathrm{n}} \equiv \frac{1}{2}\left[\frac{\mathrm{BR}(B_d^0 \to \pi^- K^+) + \mathrm{BR}(\bar{B}_d^0 \to \pi^+ K^-)}{\mathrm{BR}(B_d^0 \to \pi^0 K^0) + \mathrm{BR}(\bar{B}_d^0 \to \pi^0 \bar{K}^0)}\right] \stackrel{\mathrm{Exp}}{=} 0.79 \pm 0.08, \quad (111)$$

where the EW penguin contributions enter in colour-allowed form through the decays with π^0-mesons in the final states. Theoretically, the EW penguin effects are described by the following parameters:

$$q \stackrel{\mathrm{SM}}{=} 0.69, \quad \phi \stackrel{\mathrm{SM}}{=} 0^\circ. \quad (112)$$

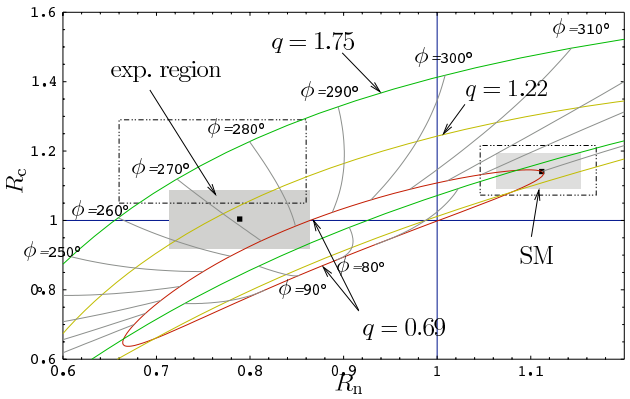

Figure 10. The situation in the R_n–R_c plane, as discussed in the text.

Here q, which can be calculated in the SM with the help of the $SU(3)$ flavour symmetry,[120] measures the "strength" of the EW penguins with respect to the tree contributions, and ϕ is a CP-violating weak phase with an origin lying beyond the SM. EW penguin topologies offer an interesting avenue for NP to manifest itself, as is already known for several years.[121,122]

In Fig. 10, we have shown the current situation in the R_n–R_c plane: the experimental ranges and those predicted in the SM are indicated in grey, and the dashed lines serve as a reminder of the corresponding ranges in Ref. 42; the central values for the SM prediction have hardly moved, while their uncertainties have been reduced a bit. Moreover, we show contours for values of $q = 0.69$, $q = 1.22$ and $q = 1.75$, with $\phi \in [0°, 360°]$. We observe that we arrive no longer at a nice agreement between our SM predictions and the experimental values. However, as becomes obvious from the contours in Fig. 10, this discrepancy can be resolved if we allow for NP in the EW penguin sector, i.e. keep q and ϕ as free parameters. Following these lines, the successful picture described above would not be disturbed, and we obtain full agreement between the theoretical values of $R_{n,c}$ and the data. The corresponding values of q and ϕ are given as follows:

$$q = 1.08\,^{+0.81}_{-0.73}, \quad \phi = -(88.8^{+13.7}_{-19.0})°, \tag{113}$$

where in particular the large CP-violating phase would be a striking signal of NP. These parameters allow us then to predict also the CP-violating observables of the $B^\pm \to \pi^0 K^\pm$ and $B_d \to \pi^0 K_S$ decays,[30] which should provide useful tests of this scenario in the future. Particularly promising in this respect are rare K and B decays.

8.4. *Step III: Rare K and B Decays*

In order to explore the implications for rare K and B decays, we assume that NP enters the EW penguin sector through enhanced Z^0 penguins with a new CP-violating phase. This scenario, which belongs to class C introduced in Subsection 5.2, was already considered in the literature, where model-independent analyses and studies within SUSY were presented.[123,124] In our strategy, we determine the short-distance function C characterizing the Z^0 penguins through the $B \to \pi K$ data. Performing a renormalization-group analysis,[109] we obtain

$$C(\bar{q}) = 2.35\ \bar{q}e^{i\phi} - 0.82 \quad \text{with} \quad \bar{q} = q\left[\frac{|V_{ub}/V_{cb}|}{0.086}\right]. \tag{114}$$

If we evaluate then the relevant box-diagram contributions within the SM and use (114), we can calculate the short-distance functions

$$X = 2.35\ \bar{q}e^{i\phi} - 0.09 \quad \text{and} \quad Y = 2.35\ \bar{q}e^{i\phi} - 0.64, \tag{115}$$

which govern the rare K, B decays with $\nu\bar{\nu}$ and $\ell^+\ell^-$ in the final states, respectively. In the SM, we have $C = 0.79$, $X = 1.53$ and $Y = 0.98$, with *vanishing* CP-violating phases.

Table 1. Comparison of the predicted values of $R_{\rm c}$ and $R_{\rm n}$ taking the constraints from rare decays into account with the evolution of the data, as discussed in the text.

	"Old" data	Prediction with RDs	"New" data
$R_{\rm c}$	1.17 ± 0.12	$1.00^{+0.12}_{-0.08}$	1.00 ± 0.08
$R_{\rm n}$	0.76 ± 0.10	$0.82^{+0.12}_{-0.11}$	0.79 ± 0.08

If we impose constraints from the data for rare decays, in particular those on $|Y|$ following from $B \to X_s\mu^+\mu^-$, the following picture arises:

$$\bar{q} = 0.92^{+0.07}_{-0.05}, \quad \phi = -(85^{+11}_{-14})^\circ. \tag{116}$$

In Table 1, we compare the corresponding predictions of $R_{\rm c}$ and $R_{\rm n}$ with the "old" data, which were available when these predictions were made,[42] and the "new" data, which emerged at the ICHEP '04 conference.[102] We observe that the data have moved accordingly.

The values in (116) are compatible with all the current data on rare decays, and are in accordance with the new $B \to \pi K$ data. However, we may still encounter significant deviations from the SM expectations for

certain rare decays, with a set of predictions that is characteristic for our specific NP scenario, thereby allowing an experimental *test* of this picture. The most spectacular effects are the following ones:

- $\mathrm{BR}(K_\mathrm{L} \to \pi^0 \nu\bar{\nu})$ is enhanced by a factor of $O(10)$, which brings it close to the Grossman–Nir bound,[125] whereas $\mathrm{BR}(K^+ \to \pi^+ \nu\bar{\nu})$ remains essentially unchanged. Consequently, we would also have a strong violation of the following MFV relation:[126]

$$\underbrace{(\sin 2\beta)_{\pi\nu\bar{\nu}}}_{-(0.69^{+0.23}_{-0.41})} = \underbrace{(\sin 2\beta)_{\psi K_\mathrm{S}}}_{+(0.725 \pm 0.037)} \quad , \tag{117}$$

  where we have indicated the corresponding numerical values.
- The decay $K_\mathrm{L} \to \pi^0 e^+ e^-$ would now be governed by direct CP violation, and its branching ratio would be enhanced by a factor of $O(3)$. The interesting implicatios for $K_\mathrm{L} \to \pi^0 \mu^+ \mu^-$ were discussed in a recent paper.[127]
- In the case of $B_d \to K^* \mu^+ \mu^-$, an integrated forward–backward CP asymmetry[124] can be very large, whereas it vanishes in the SM. The corresponding NP effects for the lepton polarization asymmetries of $B \to X_s \ell^+ \ell^-$ decays were recently studied.[128]
- The branching ratios for $B \to X_{s,d} \nu\bar{\nu}$ and $B_{s,d} \to \mu^+ \mu^-$ decays would be enhanced by factors of 2 and 5, respectively, whereas the impact on $K_\mathrm{L} \to \mu^+ \mu^-$ is rather moderate.

If future, more accurate, $B \to \pi\pi, \pi K$ data will not significantly modify the currently observed patterns in these decays, the scenario of enhanced Z^0 penguins with a large CP-violating NP phase ϕ will remain an attractive scenario for physics beyond the SM. It will then be very interesting to confront the corresponding predictions for the rare K and B decays listed above with experimental results.

9. Conclusions and Outlook

Flavour physics offers interesting strategies to explore the SM and to search for signals of NP. In the B-meson system, data from the e^+e^- B factories agree on the one hand remarkably well with picture of the Kobayashi–Maskawa mechanism, where the accordance between the measurement of $\sin 2\beta$ through $B_d \to J/\psi K_\mathrm{S}$ decays and the CKM fits is the most important example. On the other hand, there are also hints for discrepancies with the SM, and it will be very interesting to monitor these effects in the future.

Despite this impressive progress, there are still regions of the B-physics "landscape" left that are unexplored. For instance, $b \to d$ penguin processes are now close to enter the stage, since lower bounds for the corresponding branching ratios that can be derived in the SM are found to be close to the current experimental upper limits.[129] In fact, the BaBar collaboration has already reported the first signals for the $B_d \to K^0 \bar{K}^0$ channel, in accordance with these bounds.[130] The lower SM bounds for other non-leptonic decays of this kind and for $B \to \rho\gamma$ transitions suggest that these modes should also be observed soon. For the more distant future, decays such as $B \to \rho \ell^+ \ell^-$ decays are left. Since the various $b \to d$ penguin modes are governed by different operators, they may be affected differently by NP. Moreover, as we have emphasized throughout these lectures, also the B_s-meson system is still essentially unexplored, and offers a very promising physics potential for the search of NP, which should be fully exploited – after first steps at run II of the Tevatron – at the LHC, in particular by LHCb.

These studies can nicely be complemented through the kaon system, which governed the stage of CP violation for more than 35 years. The future lies now on rare decays, in particular on the $K \to \pi\nu\bar{\nu}$ modes, and any effort should be made to measure these very challenging – but also very rewarding – decays; this is the goal of the NA48 (CERN), E391(a) (KEK/J-PARC) and KOPIO (BNL) experiments.

In addition to these electrifying aspects, flavour physics offers many more exciting topics, which we could unfortunately not cover here. Important examples are the D-meson system, electric dipole moments, and the search for flavour-violating charged lepton decays.

For the search of NP and the exploration of its nature, it is important to keep an eye on all of these processes and to aim for the *whole* picture. In particular correlations between various K and B decays play an outstanding rôle in this context, as we have illustrated through the discussion of the $B \to \pi K$ puzzle. A fruitful interplay between flavour physics and the direct NP searches by ATLAS and CMS at the LHC is also expected, and will soon be explored in much more detail.[131] I have no doubt that an exciting future is ahead of us!

Acknowledgments

I would like to thank the organizers for inviting me to this wonderful Winter Institute in such a spectacular environment, and would also like to thank the participants for their stimulating interest in my lectures.

References

1. J.H. Christenson *et al.*, *Phys. Rev. Lett.* **13**, 138 (1964).
2. V. Fanti *et al.* [NA48 Collaboration], *Phys. Lett.* **B465**, 335 (1999); A. Alavi-Harati *et al.* [KTeV Collaboration], *Phys. Rev. Lett.* **83**, 22 (1999).
3. L. Wolfenstein, *Phys. Rev. Lett.* **13**, 562 (1964).
4. J.R. Batley *et al.* [NA48 Collaboration], *Phys. Lett.* **B544**, 97 (2002); A. Alavi-Harati *et al.* [KTeV Collaboration], *Phys. Rev.* **D67**, 012005 (2003).
5. For a recent review, see A.J. Buras and M. Jamin, *JHEP* **0401**, 048 (2004).
6. B. Aubert *et al.* [BaBar Collaboration], *Phys. Rev. Lett.* **87**, 091801 (2001); K. Abe *et al.* [Belle Collaboration], *Phys. Rev. Lett.* **87**, 091802 (2001).
7. A.B. Carter and A.I. Sanda, *Phys. Rev. Lett.* **45**, 952 (1980); *Phys. Rev.* **D23**, 1567 (1981); I.I. Bigi and A.I. Sanda, *Nucl. Phys.* **B193**, 85 (1981).
8. B. Aubert *et al.* [BaBar Collaboration], *Phys. Rev. Lett.* **93**, 131801 (2004); Y. Chao *et al.* [Belle Collaboration], *Phys. Rev. Lett.* **93**, 191802 (2004).
9. N. Cabibbo, *Phys. Rev. Lett.* **10**, 531 (1963).
10. M. Kobayashi and T. Maskawa, *Prog. Theor. Phys.* **49**, 652 (1973).
11. G. Altarelli, *Nucl. Phys. (Proc. Suppl.)* **143**, 470 (2005).
12. R. Kolb, lectures given at this institute (these proceedings).
13. A.D. Sakharov, *JETP Lett.* **5**, 24 (1967).
14. W. Buchmüller, R.D. Peccei and T. Yanagida, hep-ph/0502169.
15. A.J. Buras, hep-ph/0402191.
16. A.J. Buras and R. Fleischer, *Adv. Ser. Direct. High Energy Phys.* **15**, 65 (1998).
17. R. Fleischer, hep-ph/0405091.
18. Y. Nir, hep-ph/0109090.
19. G. Branco, L. Lavoura and J. Silva, *CP Violation*, International Series of Monographs on Physics 103, Oxford Science Publications (Clarendon Press, Oxford, 1999).
20. I.I. Bigi and A. I. Sanda, *CP Violation*, Cambridge Monographs on Particle Physics, Nuclear Physics and Cosmology (Cambridge University Press, Cambridge, 2000).
21. K. Kleinknecht, *Springer Tracts in Modern Physics*, Vol. **195** (2004).
22. For a review, see A.A. Petrov, *Nucl. Phys. (Proc. Suppl.)* **B142**, 333 (2005).
23. For a recent review, see M. Pospelov and A. Ritz, hep-ph/0504231.
24. For a recent analysis, see P.H. Chankowski, J.R. Ellis, S. Pokorski, M. Raidal and K. Turzynski, *Nucl. Phys.* **B690**, 279 (2004).
25. S.L. Glashow, J. Iliopoulos and L. Maiani, *Phys. Rev.* **D2**, 1285 (1970).
26. S. Eidelman *et al.* [Particle Data Group], *Phys. Lett.* **B592**, 1 (2004).
27. L. Wolfenstein, *Phys. Rev. Lett.* **51**, 1945 (1983).
28. A.J. Buras, M.E. Lautenbacher and G. Ostermaier, *Phys. Rev* **D50**, 3433 (1994).
29. A.J. Buras, F. Schwab and S. Uhlig, hep-ph/0405132.
30. A.J. Buras, R. Fleischer, S. Recksiegel and F. Schwab, hep-ph/0410407.
31. *CKMfitter* Group: `http://ckmfitter.in2p3.fr/`; *UTfit* Collaboration: `http://utfit.roma1.infn.it/`.

32. M. Lefebvre, lectures given at this institute (these proceedings).
33. A.G. Akeroyd *et al.* [SuperKEKB Physics Working Group], hep-ex/0406071; J. Hewett *et al.*, hep-ph/0503261.
34. G. Buchalla, A.J. Buras and M.E. Lautenbacher, *Rev. Mod. Phys.* **68**, 1125 (1996); A.J. Buras, hep-ph/9806471.
35. T. Inami and C.S. Lim, *Prog. Theor. Phys.* **65**, 297 [E: **65**, 1772] (1981).
36. A.J. Buras and J.-M. Gérard, *Nucl. Phys.* **B264**, 371 (1986); A.J. Buras, J.-M. Gérard and R. Rückl, *Nucl. Phys.* **B268**, 16 (1986).
37. J.D. Bjorken, *Nucl. Phys. (Proc. Suppl.)* **B11**, 325 (1989); M. Dugan and B. Grinstein, *Phys. Lett.* **B255**, 583 (1991); H.D. Politzer and M.B. Wise, *Phys. Lett.* **B257**, 399 (1991).
38. M. Beneke, G. Buchalla, M. Neubert and C. Sachrajda, *Phys. Rev. Lett.* **83**, 1914 (1999); *Nucl. Phys.* **B591**, 313 (2000); *Nucl. Phys.* **B606**, 245 (2001).
39. H.-n. Li and H.L. Yu, *Phys. Rev.* **D53**, 2480 (1996); Y.Y. Keum, H.-n. Li and A.I. Sanda, *Phys. Lett.* **B504**, 6 (2001); Y.Y. Keum and H.-n. Li, *Phys. Rev.* **D63**, 074006 (2001).
40. C.W. Bauer, D. Pirjol and I.W. Stewart, *Phys. Rev. Lett.* **87**, 201806 (2001); C.W. Bauer, B. Grinstein, D. Pirjol and I.W. Stewart, *Phys. Rev.* **D67**, 014010 (2003).
41. A. Khodjamirian, *Nucl. Phys.* **B605**, 558 (2001); A. Khodjamirian, T. Mannel and B. Melic, *Phys. Lett.* **B571**, 75 (2003).
42. A.J. Buras, R. Fleischer, S. Recksiegel and F. Schwab, *Phys. Rev. Lett.* **92**, 101804 (2004); *Nucl. Phys.* **B697**, 133 (2004).
43. A. Ali, E. Lunghi and A.Y. Parkhomenko, *Eur. Phys. J.* **C36**, 183 (2004).
44. C.W. Bauer, D. Pirjol, I.Z. Rothstein and I.W. Stewart, *Phys. Rev.* **D70**, 054015 (2004).
45. C.W. Chiang, M. Gronau, J.L. Rosner and D.A. Suprun, *Phys. Rev.* **D70**, 034020 (2004).
46. For a review, see A.J. Buras and M. Misiak, *Acta Phys. Polon.* **B33**, 2597 (2002).
47. G. Buchalla, A.J. Buras and M.K. Harlander, *Nucl. Phys.* **B349**, 1 (1991).
48. A.J. Buras and M.K. Harlander, *Adv. Ser. Direct. High Energy Phys.* **10**, 58 (1992).
49. A. Ali, hep-ph/0412128; G. Isidori, *AIP Conf. Proc.* **722**, 181 (2004); T. Hurth, *Rev. Mod. Phys.* **75**, 1159 (2003).
50. P. Ball *et al.*, hep-ph/0003238.
51. G. Buchalla and A.J. Buras, *Nucl. Phys.* **B548**, 309 (1999).
52. G. Buchalla and A.J. Buras, *Nucl. Phys.* **B400**, 225 (1993).
53. M. Misiak and J. Urban, *Phys. Lett.* **B451**, 161 (1999).
54. A.J. Buras, *Acta Phys. Polon.* **B34**, 5615 (2003).
55. A.J. Buras, hep-ph/0101336.
56. V.M. Abazov *et al.* [D0 Collaboration], *Phys. Rev. Lett.* **94**, 071802 (2005).
57. B. Aubert *et al.* [BaBar Collaboration], hep-ex/0408096.
58. M. Battaglia *et al.*, hep-ph/0304132.
59. A.J. Buras, *Phys. Lett.* **B566**, 115 (2003).
60. J.R. Ellis, K.A. Olive and V.C. Spanos, hep-ph/0504196.

61. R. Fleischer, *Phys. Rep.* **370**, 537 (2002).
62. R. Fleischer and T. Mannel, *Phys. Lett.* **B506**, 311 (2001).
63. R. Fleischer, G. Isidori and J. Matias, *JHEP* **0305**, 053 (2003).
64. R. Fleischer and T. Mannel, *Phys. Lett.* **B511**, 240 (2001).
65. T. Goto *et al.*, *Phys. Rev.* **D70**, 035012 (2004).
66. S. Jäger and U. Nierste, *Eur. Phys. J.* **C33**, S256 (2004).
67. M. Ciuchini, E. Franco, A. Masiero and L. Silvestrini, *eConf* **C0304052**, WG307 (2003) [*J. Korean Phys. Soc.* **45**, S223 (2004)].
68. P. Ball, S. Khalil and E. Kou, *Phys. Rev.* **D69**, 115011 (2004).
69. P. Ko, *J. Korean Phys. Soc.* **45**, S410 (2004).
70. E. Gabrielli, K. Huitu and S. Khalil, hep-ph/0504168.
71. P. Ball, J.M. Frere and J. Matias, *Nucl. Phys.* **B572**, 3 (2000); P. Ball and R. Fleischer, *Phys. Lett.* **B475**, 111 (2000).
72. A.J. Buras, M. Spranger and A. Weiler, *Nucl. Phys.* **B660**, 225 (2003); A.J. Buras, A. Poschenrieder, M. Spranger and A. Weiler, *Nucl. Phys.* **B678**, 455 (2004); K. Agashe, G. Perez and A. Soni, *Phys. Rev. Lett.* **93**, 201804 (2004) and *Phys. Rev.* **D71**, 016002 (2005).
73. V. Barger, C.W. Chiang, J. Jiang and P. Langacker, *Phys. Lett.* **B596**, 229 (2004); V. Barger, C.W. Chiang, P. Langacker and H.S. Lee, *Phys. Lett.* **B598**, 218 (2004).
74. S.R. Choudhury, N. Gaur, A. Goyal and N. Mahajan, *Phys. Lett.* **B601**, 164 (2004); A.J. Buras, A. Poschenrieder and S. Uhlig, hep-ph/0410309.
75. W.S. Hou, M. Nagashima and A. Soddu, hep-ph/0503072.
76. R. Fleischer, *Eur. Phys. J.* **C10**, 299 (1999).
77. B. Aubert *et al.* [BaBar Collaboration], hep-ex/0408127.
78. K. Abe *et al.* [Belle Collaboration], *Phys. Rev.* **D71**, 072003 (2005).
79. The *Heavy Flavor Averaging Group*: `http://www.slac.stanford.edu/xorg/hfag/index.html`.
80. H. Boos, T. Mannel and J. Reuter, *Phys. Rev.* **D70**, 036006 (2004).
81. R. Fleischer and J. Matias, *Phys. Rev.* **D66**, 054009 (2002).
82. B. Aubert *et al.* [BaBar Collaboration], *Phys. Rev.* **D 71**, 032005 (2005).
83. R. Fleischer, *Nucl. Phys.* **B671**, 459 (2003).
84. For a recent review, see A. Lenz, hep-ph/0412007.
85. I. Dunietz, *Phys. Rev.* **D52**, 3048 (1995).
86. R. Fleischer and I. Dunietz, *Phys. Rev.* **D55**, 259 (1997); *Phys. Lett.* **B387**, 361 (1996).
87. A.S. Dighe, I. Dunietz and R. Fleischer, *Eur. Phys. J.* **C6**, 647 (1999).
88. D. Acosta *et al.* [CDF Collaboration], *Phys. Rev. Lett.* **94**, 101803 (2005).
89. D0 conference note 4557 (2005).
90. A. Dighe, I. Dunietz, H. Lipkin and J. Rosner, *Phys. Lett.* **B369**, 144 (1996).
91. R. Fleischer, *Phys. Rev.* **D60**, 073008 (1999).
92. Y. Nir and D.J. Silverman, *Nucl. Phys.* **B345**, 301 (1990).
93. I. Dunietz, R. Fleischer and U. Nierste, *Phys. Rev.* **D63**, 114015 (2001).
94. D. London and R.D. Peccei, *Phys. Lett.* **B223**, 257 (1989); N.G. Deshpande and J. Trampetic, *Phys. Rev.* **D41**, 895 and 2926 (1990); J.-M. Gérard and W.-S. Hou, *Phys. Rev.* **D43**, 2909; *Phys. Lett.* **B253**, 478 (1991).

95. R. Fleischer, *Z. Phys.* **C62**, 81 (1994).
96. N.G. Deshpande and X.-G. He, *Phys. Lett.* **B336**, 471 (1994).
97. R. Fleischer, *Int. J. Mod. Phys.* **A12**, 2459 (1997).
98. Y. Grossman and M.P. Worah, *Phys. Lett.* **B395**, 241 (1997).
99. D. London and A. Soni, *Phys. Lett.* **B407**, 61 (1997).
100. Y. Grossman, Z. Ligeti, Y. Nir and H. Quinn, *Phys. Rev.* **D68**, 015004 (2003).
101. `http://conferences.fnal.gov/lp2003/`.
102. `http://ichep04.ihep.ac.cn/`.
103. B. Aubert *et al.* [BaBar Collaboration], hep-ex/0408072, hep-ex/0502019.
104. K. Abe *et al.* [Belle Collaboration], hep-ex/0409049; hep-ex/0504023.
105. A.J. Buras and R. Fleischer, *Eur. Phys. J.* **C16**, 97 (2000).
106. M. Beneke and M. Neubert, *Nucl. Phys.* **B675**, 333 (2003).
107. T. Yoshikawa, *Phys. Rev.* **D68**, 054023 (2003).
108. M. Gronau and J.L. Rosner, *Phys. Lett.* **B572**, 43 (2003).
109. A.J. Buras, R. Fleischer, S. Recksiegel and F. Schwab, *Eur. Phys. J.* **C32**, 45 (2003).
110. S. Mishima and T. Yoshikawa, *Phys. Rev.* **D70**, 094024 (2004).
111. G. Buchalla and A.S. Safir, hep-ph/0406016.
112. Y.Y. Keum and A.I. Sanda, *eConf* **C0304052**, WG420 (2003).
113. B. Aubert *et al.* [BaBar Collaboration], hep-ex/0412037.
114. K. Abe *et al.* [Belle Collaboration], hep-ex/0408101.
115. R. Fleischer, *Phys. Lett.* **B459**, 306 (1999); *Eur. Phys. J.* **C16**, 87 (2000).
116. R. Fleischer and T. Mannel, *Phys. Rev.* **D57**, 2752 (1998).
117. R. Fleischer, *Eur. Phys. J.* **C6**, 451 (1999).
118. M. Neubert, *JHEP* **9902**, 014 (1999).
119. A.J. Buras and R. Fleischer, *Eur. Phys. J.* **C11**, 93 (1999).
120. M. Neubert and J.L. Rosner, *Phys. Lett.* **B441**, 403 (1998); *Phys. Rev. Lett.* **81**, 5076 (1998).
121. R. Fleischer and T. Mannel, hep-ph/9706261.
122. Y. Grossman, M. Neubert and A.L. Kagan, *JHEP* **9910**, 029 (1999).
123. A.J. Buras, and L. Silvestrini, *Nucl. Phys.* **B546**, 299 (1999); A.J. Buras *et al.*, *Nucl. Phys.* **B566**, 3 (2000); A.J. Buras, T. Ewerth, S. Jäger and J. Rosiek, *Nucl. Phys.* **B714**, 103 (2005).
124. G. Buchalla, G. Hiller and G. Isidori, *Phys. Rev.* **D63**, 014015 (2001); D. Atwood and G. Hiller, hep-ph/0307251.
125. Y. Grossman and Y. Nir, *Phys. Lett.* **B398**, 163 (1997).
126. G. Buchalla and A.J. Buras, *Phys. Lett.* **B333**, 221 (1994).
127. G. Isidori, C. Smith and R. Unterdorfer, *Eur. Phys. J.* **C36**, 57 (2004).
128. S. Rai Choudhury, N. Gaur and A.S. Cornell, *Phys. Rev.* **D70**, 057501 (2004).
129. R. Fleischer and S. Recksiegel, *Eur. Phys. J.* **C38**, 251 (2004); *Phys. Rev.* **D71**, 051501 (R) (2005).
130. B. Aubert *et al.* [BaBar Collaboration], hep-ex/0408080.
131. This topic will be addressed at a future dedicated workshop: `http://mlm.home.cern.ch/mlm/FlavLHC.html`.